AMERICAN MUSEUM
Novitates

PUBLISHED BY THE AMERICAN MUSEUM OF NATURAL HISTORY
CENTRAL PARK WEST AT 79TH STREET, NEW YORK, NY 10024
Number 3637, 49 pp., 28 figures, 1 table December 31, 2008

The Lithogeninae (Siluriformes, Loricariidae): Anatomy, Interrelationships, and Description of a New Species

SCOTT A. SCHAEFER[1] AND FRANCISCO PROVENZANO[2]

ABSTRACT

A new species of the loricariid genus *Lithogenes* Eigenmann, 1909, is described on the basis of 84 specimens captured from a single locality in the upper Río Orinoco drainage of southern Venezuela. The new species is only the third representative of the subfamily Lithogeninae to be recognized in the 100 years since the discovery of the type species, *L. villosus*, and is the only lithogenine known from more than a handful of specimens. This new material provides the basis for a comprehensive review of lithogenine systematics, comparative anatomy, and interrelationships. *Lithogenes wahari*, new species, shares with its congeners the dermal plates of the trunk comprised of three paired series, presence of a bifurcate levator arcus palatini crest and expanded lateral lamina of the hyomandibula, and the palatine sesamoid not reaching the nasal capsule, thus confirming its placement in *Lithogenes* among the Loricariidae. The new species is diagnosed among congeners by the absence of odontodes on the proximal portion of the ventral surface of the first pelvic-fin ray (vs. ventral pad covered with embedded odontodes along entire length) and thickened skin of the pelvic pad forming extensive ridges; accessory premaxillary teeth absent; anal fin with intense pigment band along base and diffuse spot at midlength of fin rays (vs. pigment band at base absent, fin rays dusky, without distinct spot). Characters useful for distinguishing lithogenine species are reviewed; revised diagnoses and descriptions are provided for the two previously described species in light of new character evidence. A detailed comparative analysis of the osteology and myology of *L. wahari* is presented and discussed relative to homologous conditions observed more broadly among the loricarioid catfishes. Of particular importance are aspects of musculoskeletal anatomy that are hitherto unknown for lithogenines, and aspects of sexual dimorphism and the anatomy of the reproductive and digestive systems that are unique or unusual among loricariid catfishes. A phylogenetic analysis of relationships among species based on morphological characters places the two Guyana Shield species (*L. villosus* and *L.wahari*) as

[1] Division of Vertebrate Zoology, American Museum of Natural History (schaefer@amnh.org).
[2] Instituto Zoología Tropical, Universidad Central de Venezuela (francisco.provenzano@ciens.ucv.ve).

 ISSN 0003-0082

sister taxa on the basis of four synapomorphies. Both species share reduction in the width and extent of the jaws, resulting in the derived reduction in the numbers of teeth carried by the jaw elements. Evaluated with respect to the geographic distribution of the species, the pattern of phylogenetic relationships suggests an ancestral widespread distribution for the Lithogeninae throughout the Guyana Shield plus the Caribbean and eastern Andean foreland basin of northern South America, followed by vicariance and subsequent divergence of populations now isolated in the coastal mountains of northern Venezuela and the Guyana Shield region. Lithogenine catfishes share a number of unique features with astroblepid catfishes that are not observed to occur in other members of the Loricariidae, such as the morphology of the pelvic fins, specialized pelvic musculature, and associated adaptations for climbing. Evaluated against the evidence supporting their phylogenetic placement as the sister group to all other Loricariidae, exclusive of the Astroblepidae, these shared similarities suggest that the association with rocky habitats of headwater stream systems and the ability to climb vertical surfaces may represent ancestral conditions for the lineage leading to the astroblepid plus loricariid catfishes.

INTRODUCTION

Loricariid catfishes of the genus *Lithogenes* (subfamily Lithogeninae; Reis et al., 2003) are among the most distinctive members of the family and are represented at present by two species, the type species *L. villosus* Eigenmann, 1909, from Guyana and *L. valencia* Provenzano et al., 2003, from Venezuela. Published information regarding these fishes is limited, in part because these species are known from the sum total of nine specimens. *Lithogenes villosus* was described from a single specimen collected in 1908 and subsequently two additional specimens (AUM 28152) were obtained from near the type locality in 1998 (Hardman et al., 2002); otherwise, no material of this species had been discovered in the 90 years between these two events. *Lithogenes valencia* is known from six specimens collected from a single locality in northern Venezuela. Its type locality is situated in a heavily populated and industrialized region of the Lago Valencia drainage and, despite extensive survey work in the area, no additional specimens of this species are known (Provenzano et al., 2003).

Aspects of the anatomy of *Lithogenes villosus* and its phylogenetic relationships among loricarioid catfishes were addressed in Schaefer (2003). That study, based on parsimony analysis of 41 morphological characters drawn from internal and external features of the holotype, concluded that *Lithogenes* represents the sister group of all other members of the family Loricariidae, exclusive of the family Astroblepidae. The peculiar morphology of lithogenine loricariids (e.g., having a nearly naked body, with plates extremely reduced; modified pelvic fin and associated musculature), combined with so few specimens, has contributed to the controversy about their family assignment, beginning with Gosline (1947) and promoted by Nijssen and Isbrücker (1987). Lithogenine morphology was characterized by Schaefer (2003) as a mosaic of autapomorphic and plesiomorphic features, with the numerous similarities between astroblepids and lithogenines represented for the most part by symplesiomorphy.

Discovery of a second *Lithogenes* species in 2003 served to confirm the generic-level distinction of these fishes relative to other loricariids. *Lithogenes* is diagnosed relative to all other loricariids by a robust suite of uniquely derived features, most notably involving specializations of the jaw suspensorial bones and reduction in the extent of dermal plates on the posterior trunk. We report herein upon a third species of *Lithogenes*, only the second to be discovered and described in the 100 years since the discovery and description of the first lithogenine, and the only species represented by more than a handful of preserved specimens. This additional material further provides an opportunity to report on a detailed treatment of the osteology and myology of the new species, an updated and enhanced overview of lithogenine systematics, and a comparative analysis of lithogenine anatomy.

The occurrence of the new species in the headwaters of the Orinoco River of southwestern Venezuela confirms a Guyana Shield plus Caribbean coastal distribution for the Lithogeninae, but sheds precious little insight

into its curious widely disjunct geographic distribution and remarkable absence of representatives from vast intervening regions across northern South America. The habitat of the new species, like that of its congeners, is in accord with the etymological derivation of the generic name (i.e., from the Greek *lithos* = rock, *gen-*=born of, or produced from) and reflects its requirement for bedrock substrates of upland, high-gradient clearwater streams. Although this habitat type is comparatively common in the diverse streams and rivers occurring throughout much of the Andean foreland and the Guyana Shield regions of northern South America, the nature of these freshwater systems and the presumed preference of these fishes for relatively small streams combine to render much of this particular habitat type rather inaccessible, except at certain times of the year when high-water conditions might prevail over extended periods. Our personal experience in the headwaters of the Río Cuao in 2001 occurred during conditions exactly opposite of that just described, namely, extreme low water that precluded rapid upstream travel and severely limited the extent of our river surveys. In fact, it was only after three focused expeditions to the western Guyana Shield drainages of Venezuela, two of which were directed to the Cuao region, that the new species was finally discovered, following earlier anecdotal reports of the existence of populations of a strange ''unplated'' loricariid and a poorly preserved specimen obtained from Dr. Stanford Zent, an anthropologist working with indigenous peoples of Amazonas State.

As will become evident below, lithogenine loricariids possess a number of morphologies that are seemingly related to climbing and adhesion to solid surfaces. In addition to having the ventral mouth with expanded lips forming a suckerlike disk and numerous enlarged odontodes on the surfaces of the fin rays contacting the substratum that are useful in adhesion in lotic conditions that are also found in other members of the family (Bhatti, 1938; Macdonnell and Blake, 1990), lithogenines have a specialized pelvic fin and musculature that function to assist in adhesion as well as in vertical propulsion, or climbing. The latter activity is made possible by the specialized protractor ischii muscle of the pelvic fin that in lithogenines is completely separate from the hypaxialis musculature. Alternating contractions of this muscle, along with the antagonist retractor ischii, coupled with a grasping pelvic fin and pelvic girdle that is loosely slung via its pivot at the lateropterygium bone, cause the entire pelvic girdle to slide anteroposteriorly relative to the mouth and trunk. When combined with successive and alternating attachments to the substratum via the oral sucking disk and pevic fins, the fishes are able to progress forward and even vertically over a surface much like an inchworm (Evermann and Kendall, 1905; Johnson, 1912). Interestingly, however, these homologous morphologies and behaviors occur in the Andean astroblepid catfishes and are not observed in other members of the Loricariidae.

In this work, we describe a new species of *Lithogenes* and review and rediagnose the two established species in light of the discovery of new characters exhibited by the new species. Because of the relative basal phylogenetic position of *Lithogenes* among the members of the Loricariidae, and because the new species is the only lithogenine known from numerous preserved specimens, we present a detailed osteological and myological treatment of the new species in order to provide a baseline for future taxonomic and phylogenetic studies.

Of particular importance are aspects of musculoskeletal anatomy that are hitherto unknown for lithogenines, and aspects of sexual dimorphism and the anatomy of the reproductive and digestive systems that are unique or unusual among loricariid catfishes.

METHODS

Counts and measurements follow Provenzano et al. (2003). Counts of pectoral-fin rays, ribs, and vertebrae were obtained from radiographs using a Faxitron cabinet radiograph system and Kodak Industrex M100 film. For counts that vary among specimens, the condition observed in the holotype is denoted by an asterisk (*). Osteological preparations were made following Taylor and Van Dyke (1985). Specimens prepared for myological examination

were lightly stained in a solution of 70% ethanol and alizarin red-S following Springer and Johnson (2000). Nomenclature for cranial bones follows Schaefer (1987, 1997); terminology for bones of the caudal skeleton follows Lundberg and Baskin (1969). Muscle terminology generally follows Shelden (1937), Winterbottom (1974), and Springer and Johnson (2004). Terminology for the cranial muscles follows Geerinckx (2007) and differs from that used in previous descriptions of loricariid myology in three notable respects. First, the muscle previously termed retractor tentaculi that inserts on the posterior maxilla margin is hypothesized to have a different developmental origin in loricariids relative to other loricarioids and siluroids and is here termed levator tentaculi. Second, the muscle originating from the posterohyal and inserting on the dentary that has been widely referred to as *protractor hyoideus* is here termed *intermandibularis posterior*. As is the condition for *Ancistrus* described by Geerinckx (2007: 110–113), in *Lithogenes* there is no transverse myocomma between the plesiomorphic separately innervated compound protractor hyoideus muscle components and, by inference, no homology with an interhyoideus muscle derivative. Whether the muscle in question is innervated by the trigeminal nerve (indicative of intermandibularis homology) or by the facial nerve (indicative of interhyoideus homology) is not determined in *Lithogenes*. Third, the muscle previously termed *retractor tentaculi* is here termed *retractor veli* following Geerinckx (2007), due to its insertion on the oral valve in *Lithogenes*.

Metric Analyses

Ten males and 10 females each were randomly selected from among the paratypes of *L. wahari* for morphometric and meristic analysis of sexual dimorphism in body shape. Sex was determined by inspection of external anatomy. Morphometric data in the form of 32 homologous geometric landmarks describing aspects of head and body shape (fig. 1) were digitized from images of each specimen. Counts of teeth and fin rays were taken for the same specimens. Standard length (SL) was measured with digital calipers and recorded to the nearest 0.1 mm. Interlandmark distances were extracted from this data for descriptive purposes and are summarized in table 1. Multivariate analysis of covariance (MANCOVA) was used to identify differences between sexes for the inter-landmark distance data. Centroid size, a generalized proxy for specimen size (Rohlf and Slice, 1990), was computed from the 15 landmarks describing bilateral head shape (fig. 1A) and used as the covariate. Homogeneity of slopes between sexes was tested over all distance variables combined and separately for each individual variable, with those variables showing significant interaction between sex and size removed from further consideration. Shape differences between sexes were described using the method of thin-plate splines and relative warps (Adams et al., 2004) on data restricted to unilateral landmarks (i.e., computed as the average of each bilateral landmark pair). Descriptive statistics and MANCOVA were generated using Systat ver. 11. Geometric morphometric computations utilized the Integrated Morphometrics Package by David Sheets (available at http://life.bio.sunysb.edu/morph).

Phylogenetic Analysis

Parsimony analysis of discrete morphological characters was performed using the programs NONA version 2.0 (Goloboff, 1999) and WinClada version 1.00.08 (Nixon, 2002). Characters were chosen based on the presence of variation among *Lithogenes* species; autapomorphies were ignored. Characters were unordered and equally weighted. Following Schaefer (2003), *Astroblepus* (Astroblepidae) and *Hemipsilichthys gobio* (Loricariidae) were included in the analyses as outgroups; relationships among both ingroup and outgroup taxa were evaluated simultaneously.

Institutional Abbreviations

AMNH	American Museum of Natural History, New York
AUM	Auburn University, Auburn, Alabama
CAS	California Academy of Sciences, San Francisco
CM	Carnegie Museum, Pittsburgh (material now mostly held at FMNH)

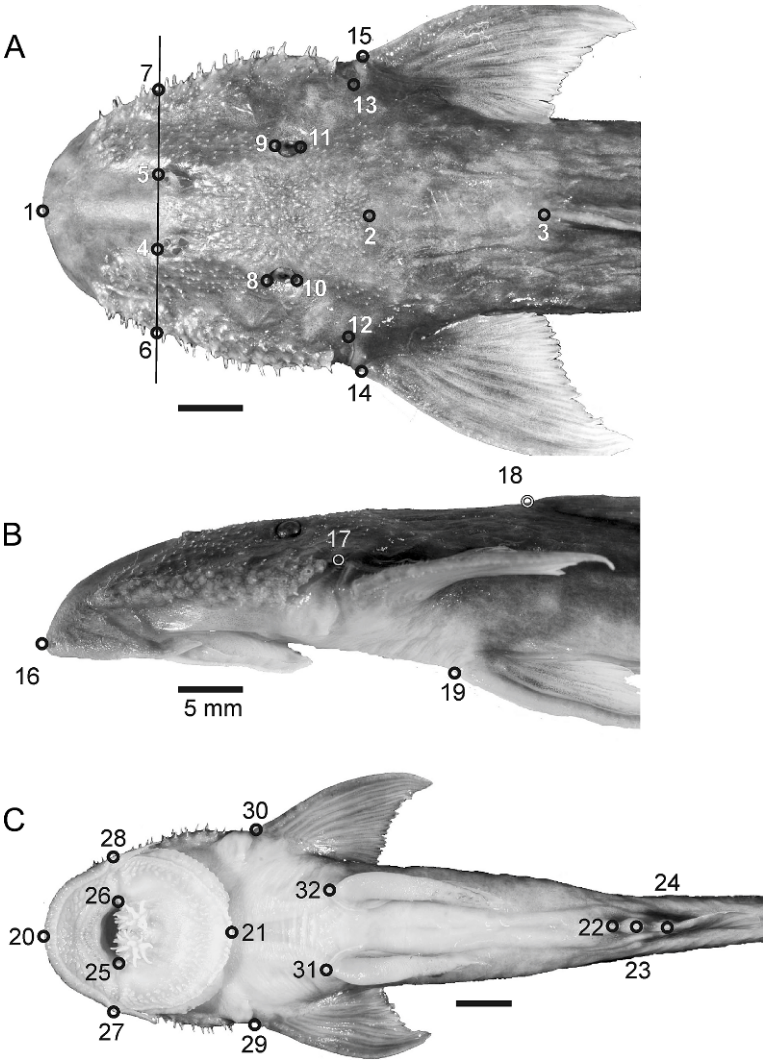

Fig. 1. Landmark coordinates digitized from images of individual specimens of *Lithogenes wahari* and used in the morphometric analyses. **A,** dorsum of head; **B,** lateral view of anterior half of body; **C,** ventral view of head and anterior trunk. Landmarks were chosen to represent homologous coordinate points among individuals and are defined by anatomical features, including points of intersection and perimeter boundary limits. Landmarks 6 and 7 were determined by the point on the perimeter of the head at which intersects a line drawn through landmarks 4 and 5. Scale bar is 5 mm.

FMNH	Field Museum of Natural History, Chicago
MBUCV	Museo de Biologia, Universidad Central de Venezuela, Caracas
MCP	Museu de Ciencias e Tecnologia, Pontificia Universidade Católica do Rio Grande do Sul, Porto Alegre, Brazil
SU	former Stanford University collections, now housed at CAS
USNM	National Museum of Natural History, Smithsonian Institution, Washington

Comparative Material Examined

Astroblepus cf. *festae*, FMNH 96627, 1 cs, Ecuador, Prov. Napo, Río Malo (Río Quijos-Coca drainage).

TABLE 1
Selected morphometrics for *Lithogenes wahari* based on inter-landmark distances computed from landmarks depicted in figure 1
Landmark pairs representing each distance variable given in parentheses. Measures are reported as percent standard length unless noted otherwise; "SD" denotes one standard deviation.

		Paratypes					
		Males (n = 10)			Females (n = 10)		
Variable (landmark pair)	Holotype	Range	Mean	SD	Range	Mean	SD
Standard length	57.2	43.7–77.5	59.9	11.0	34.6–57.2	46.3	6.8
Centroid size	–	21.3–37.9	29.5	5.5	17.5–28.8	24.1	3.7
Predorsal length (1–3)	39.5	38.6–44.9	41.3	2.2	39.5–43.5	42.5	0.9
Presupraoccipital length (1–2)	29.4	27.0–33.2	29.3	2.1	29.4–32.1	31.0	0.7
Internaris width (4–5) as %HL	17.5	15.8–20.8	18.3	1.5	16.8–22.3	18.8	1.6
Snout width (6–7) as %HL	64.9	56.0–71.9	62.9	4.6	60.3–71.1	64.4	4.0
Interorbit width (8–9) as %HL	31.7	34.8–40.8	37.8	1.9	37.6–40.8	39.1	1.1
Interopercle width (12–13) as %HL	70.4	60.3–81.5	70.8	10.2	61.1–76.4	70.5	4.8
Body width (14–15)	27.2	23.8–26.9	25.8	0.9	26.3–29.5	28.1	1.0
Orbit length (8–10) as %HL	10.2	7.3–12.1	9.9	1.6	9.4–13.2	10.7	1.1
Preorbit length (1–8) as %HL	67.3	63.9–71.5	67.6	2.8	63.8–70.3	67.0	2.4
Prenaris length (1–4) as %HL	31.4	29.8–36.9	33.0	1.9	30.5–36.9	33.6	2.0
Body depth (18–19)	18.2	15.6–19.3	17.3	1.2	17.5–19.2	18.4	0.6
Preanal-fin length (20–24)	79.8	75.8–83.1	79.3	1.9	76.8–83.7	81.2	2.3
Anus–anal-fin length (22–24)	3.9	4.8–6.4	5.6	0.6	3.6–5.7	4.3	0.7
Anus–genital papilla length (22–23)	2.1	2.4–3.2	2.6	0.3	1.6–3.1	2.4	0.4
Oral disk length (20–21) as %HL	83.5	68.8–86.3	79.4	5.5	78.6–89.7	82.6	3.9
Mouth width (25–26) as %HL	28.6	24.7–30.7	27.5	2.2	25.0–33.2	28.9	3.2
Oral disk width (27–28) as %HL	62.5	57.1–74.1	64.0	5.8	62.5–72.6	66.7	3.7
Pectoral width (29–30)	27.4	23.4–26.4	25.3	0.8	26.5–29.3	27.4	0.8
Pelvic width (31–32)	11.9	11.5–13.1	12.2	0.5	11.7–13.8	12.9	0.6
Prepectoral length (20–29)	31.6	26.5–30.6	28.8	1.2	30.8–33.7	31.8	0.8
Prepelvic length (20–31)	39.2	36.4–41.8	38.2	1.6	38.3–41.2	39.4	1.0
Pectoral to pelvic fin-origin (29–31)	12.5	12.4–14.9	13.2	0.8	11.7–13.4	12.6	0.6
Pelvic-fin origin to anus (31–24)	34.3	38.6–44.0	42.0	1.5	38.8–45.2	42.8	2.0

Astroblepus sp., USNM 302652, 3 cs, Peru: Prov. Paucartambo, Río San Pedro.
Astroblepus orientalis, ANSP 168821, 3 cs, Venezuela, Est. Merida, Rio Gonzales, tributary of Rio Chama.
Hemipsilichthys gobio, MCP 19780, 1 cs, Brazil, Rio de Janeiro, rio Preto.

SYSTEMATICS

Key to the Species of *Lithogenes*

1a. Nine or fewer teeth in the emergent row of the premaxilla; anteriormost lateral cheek plate a thin, elongate rod; lateral snout with intense dark pigment band lateral to nares from eye to maxillary barbel base; dorsal and ventral series plates on caudal peduncle large, regular in arrangement; in contact with their antimeres and with plates of the median series at least posteriorly . . . . . *L. villosus*

1b. Ten or more teeth in the emergent row of the premaxilla; all lateral cheek plates laminar; lateral snout without pigment band lateral to nares; dorsal and ventral series plates on caudal peduncle small, fragmentary, irregular in shape and position; not in contact with antimeres or with plates of median series 2

2a. Six or seven branched anal-fin rays; fleshy pad of ventral surface of first pelvic-fin ray without odontodes proximally; adipose fin without ossified spine; 12 premaxillary teeth, premaxilla accessory teeth absent . . . . . *L. wahari*, new species

2b. Five branched anal-fin rays; fleshy pad of first pelvic-fin ray with embedded odontodes along entire ventral surface; adipose fin with an ossified spine; 25–29 premaxillary teeth, premaxilla accessory teeth present. . . *L. valencia*

Fig. 2. *Lithogenes villosus*, holotype, FMNH 52960, male, 33.0 mm SL, Guyana: Aruataima Falls, upper Potaro River.

Lithogenes villosus Eigenmann, 1909
Figure 2

HOLOTYPE: FMNH 52960 (former CM 1002), male, 33.0 mm SL, Guyana: Aruataima Falls, upper Potaro River, C. H. Eigenmann, 1908.

NONTYPE MATERIAL: AUM 28152 (1: 29.5; 1 c&s: 28.0 mm SL) Guyana: Potaro River, Chenapou Cataract, 14.7 mi SW Mende's Landing, 5°00′05″N, 59°37′ 33″W, L.M. Page et al., 31 Oct. 1998.

DIAGNOSIS: The presence of eight branched pectoral-fin rays (vs. nine); single (vs. multiple) lateral cheek plate developed as a thin rod (vs. expanded, laminar); trunk plates of dorsal and ventral series large, contacting plates of midline series at least posteriorly (vs. plates small, not contacting those of midline series posteriorly); presence of a dark pigment band on snout (vs. snout region uniformly pigmented or mottled) serves to distinguish this species from all congeners. *Lithogenes villosus* is further distinguished from *L. wahari* by the presence of odontodes along entire length of the ventral surface of the first pelvic-fin ray (vs. odontodes absent from proximal portion of ventral surface); accessory premaxillary teeth present (vs. absent); anal fin dusky (vs. intense pigment band along fin base and diffuse spot at midlength of fin rays); adipose fin with an ossified spine along its leading edge (vs. spine absent). Further distinguished from *L. valencia* by the presence of asymmetrically bifid teeth (vs. tooth cusps symmetrically bifid), seven (vs. five) branched anal-fin rays.

DESCRIPTION: Body elongate, slender; head narrow, head length 34% SL, head width 22% SL and 73% HL, head depth 43% HL. Greatest body depth at dorsal-fin origin, 12% SL. Body between pelvic- and dorsal-fin origins circular in cross section, caudal peduncle elongate, slender, round in cross section; least caudal peduncle depth anterior to procurrent caudal-fin rays, 4% SL.

Eyes small, 12% HL, iris operculum absent. Pterotic with slender ventral process posterior

to opercle. Three pairs of dermal plates on lateral cheek margin between opercle and maxilla; first (anteriormost) plate elongate, slender, positioned above maxilla and above anterolateral corner of lower lip.

Premaxillary teeth 9–10, emergent dentary teeth 2–3 per jaw element; jaw teeth small, slender, cusps asymmetrically bifid; cusps of dentary teeth typically worn, blunted. Accessory premaxillary dentition present, consisting of patch of approximately 20 smaller, unicuspid, pointed teeth on jaw element located posterodorsal to emergent series of teeth within cup. Oral disk circular, ventral surface smooth except for creases along thickened, fleshy anterior margin and numerous small papillae along narrow band at posterior lip margin, fringing papillae tend to be more elongate than those located interiorly. Posterior lip margin double, consisting of thick papillose ventral layer, overlain by thinner smooth sheet of skin that extends posteriorly slightly beyond margin of ventral papillose margin. Area posterior to dentaries bearing elevated circular clump of about 20 villiform papillae (fig. 3A); contralateral papillae clumps separated from one another at midline, papillae elongate, slender, with pointed tips. Maxillary barbels present, separated from lateral lip margin.

Dorsal-fin rays i,7; first ray segmented, unbranched but not thickened, without odontodes; first dorsal-fin spinelet absent. Pectoral-fin rays i,8; first ray segmented, unbranched, and thickened, anterior edge rugose, bearing odontodes (these mostly eroded). Pelvic-fin rays i,4; first ray segmented, divided to near base, greatly thickened, flattened, with broad fleshy pad on ventral surface bearing numerous large odontodes. Anal-fin rays ii,7; first two rays segmented, unbranched, not thickened, without odontodes. Caudal-fin rays i,14,i; three dorsal and three ventral procurrent rays, odontodes present on segmented and procurrent rays. Adipose fin with thickened, well-ossified leading spine bearing numerous odontodes, fin spine attached to trunk posteriorly via low, thin membrane.

Anus tubular, located anterior to anal fin origin; genital papilla adjacent and immediately posterior to anus, globose proximally, abruptly developed into slender, pointed tip distally.

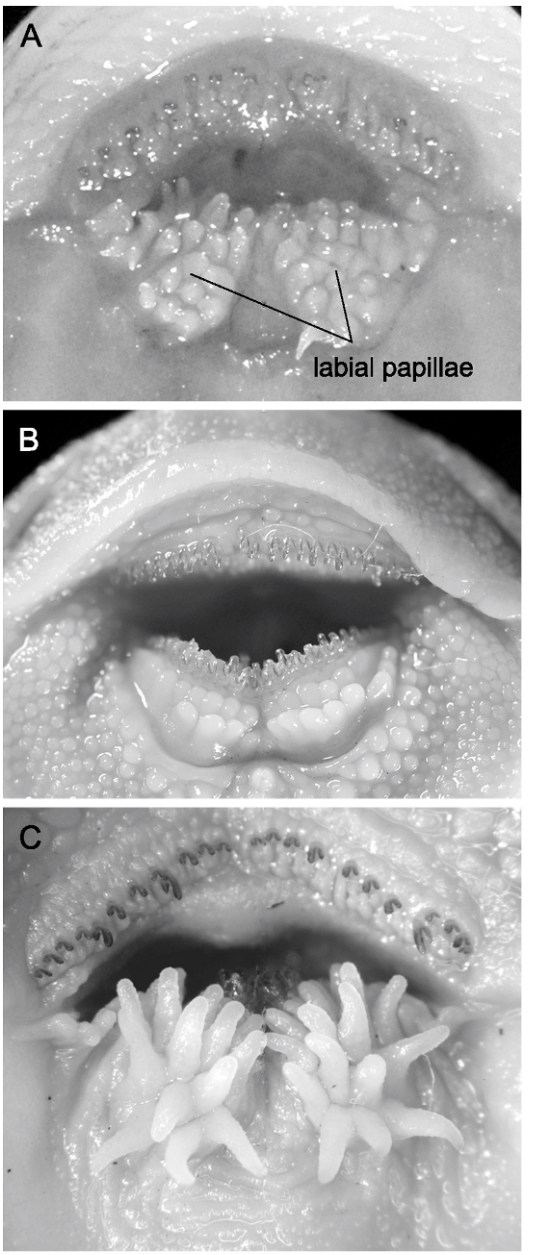

Fig. 3. Ventral surface of mouth and lower lip showing labial papillae. **A,** *L. villosus* holotype FMNH 52960; **B,** *Neoplecostomus microps*, AMNH 93230; **C,** *Lithogenes wahari* AMNH 233086.

Lateral line complete, continuous on trunk from pterotic to base of caudal fin. Three paired series of dermal plates on trunk. Median plate series bearing lateral-line canal

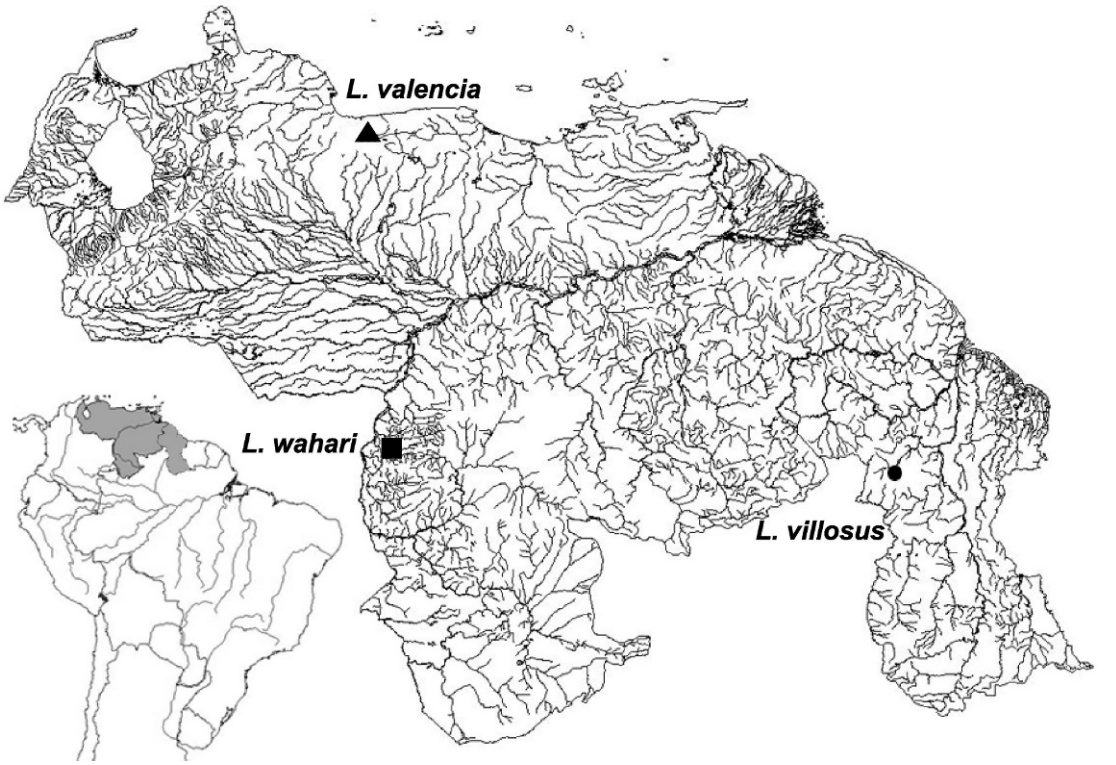

Fig. 4. Distribution of the Lithogeninae. Map of northern South America and drainage map of Venezuela and Guyana showing collection localities for *Lithogenes valencia* (triangle); *L. villosus* (circle); *L. wahari* (square).

and numbering 14 plates (left side), 13 plates (right side); plates of median series becoming progressively larger posteriorly; anteriormost plate located at vertical through anal-fin origin, posteriormost plate at caudal-fin base and overlapping proximal portion of median branched rays. Four pairs of plates in dorsal series, all bearing odontodes; one (anteriormost) unpaired plus four paired plates in ventral series, all bearing odontodes. Two unpaired plates along dorsal midline immediately in advance of adipose fin. Abdomen without plates; pectoral skeleton not exposed, covered by skin. Odontodes present on all plates; odontodes otherwise absent on head and trunk.

COLOR IN ALCOHOL: Pigmentation generally consisting of dark brown melanophores on an underlying cream-yellow ground coloration. Dorsal surface of head uniformly dusky, ventral surface unpigmented. Intense concentration of pigment in form of narrow band lateral to nares from anterior orbit margin to maxilla base. Light concentration of melanophores around nares and opercle flap. Dorsum of trunk uniformly dusky, with concentration of melanophores arranged as 5–6 diffuse, irregular blotches along midline between head and caudal fin; broad, diffuse transverse saddles anterior to dorsal fin and between dorsal fin insertion and adipose-fin origin. Fins uniformly dusky, caudal fin with concentration of melanophores at base and two diffuse, irregular vertical bands across fin rays.

DISTRIBUTION: Known only from the type locality on the upper Potaro River above Kaieteur Falls, Guyana (fig. 4).

Lithogenes valencia Provenzano et al., 2003
Figure 5

HOLOTYPE: MBUCV V-30740 (former MBUCV V-7198; former CAS 28361), 51.2 mm SL male, Venezuela, Est. Cara-

Fig. 5. *Lithogenes valencia*, holotype, MBUCV V-30740, 51.2 mm SL male, Venezuela, Estado Carabobo, Lago de Valencia basin.

bobo, Lago de Valencia basin, collector and date unknown.

PARATYPES: MBUCV V-7198 (1: 46.8; 1 c&s), CAS 28361 (2: 45.0 female, 48.5 male; 1 c&s: 44.0 female); collected with holotype.

DIAGNOSIS: The presence of five branched anal-fin rays (vs. seven); premaxilla broad, elongate (vs. narrow, short), premaxillary teeth 25–29 (vs. 9–10); tooth cusps symmetrically bifid, spatulate and tips not diverged from one another along midline (vs. cusps asymmetrically bifid, or symmetrically bifid with tips diverging from one another along midline) serves to distinguish this species from all congeners. *Lithogenes valencia* is further distinguished from *L. wahari* by presence of odontodes along entire length of the ventral surface of the first pelvic-fin ray (vs. odontodes absent from proximal portion of ventral surface); accessory premaxillary teeth present (vs. absent); anal fin dusky (vs. intense pigment band along fin base and diffuse spot at midlength of fin rays); adipose fin with an ossified spine along its anterior edge. Further distinguished from *L. villosus* by presence of nine branched pectoral-fin rays (vs. eight); first lateral cheek plate laminar, broad (vs. thin, narrow rod); trunk plates of dorsal and ventral series small, not contacting those of midline series posteriorly (vs. plates large,

contacting plates of midline series at least posteriorly); snout region uniformly pigmented or mottled (vs. presence of a dark pigment band lateral to nares).

DESCRIPTION: Head and body broad, extremely depressed. Greatest body width at posterior opercle, 27.2%–29.3% SL, 83.2%–92.8% head length (HL). Trunk broad, mid-region of trunk between pectoral-fin origin and dorsal-fin base not attenuate, not appreciably tapering posteriorly, body width at pectoral-fin base 22.0%–25.6% SL, 81.2–87.6% head width (HW). Head extremely depressed such that gill openings visible in both dorsal and ventral views; head depth at anterior orbit margin 30.0%–45.1% HL, 32.3%–54.2% HW. Snout margin bluntly rounded. Eyes small, 8.0%–10.0% HL; iris operculum absent.

Premaxillary teeth 25–29 in single emergent row on each jaw element; symmetrically bifid, cusps closely juxtaposed, separated by straight median cleft to cusp base; cusp tips smoothly rounded. Accessory premaxillary dentition present, consisting of patch of approximately 8–9 smaller, unicuspid, sharply pointed teeth on each jaw element located on medial quarter of posterior premaxilla. Dentary teeth 4–5 per jaw element; tooth and cusp shape as per emergent premaxillary dentition.

Oral disk circular; ventral surface smooth anterior to premaxilla, narrow band of elongate ridges along anterior lip margin between maxillary barbels; ridges at snout tip oriented transversely, becoming increasingly oblique posterolaterally, oriented parallel to saggital plane posterior to maxilla. Anterior margin scalloped. Area posterior to dentaries bearing elevated circular clump of villiform papillae; those located caudad most prominent; contralateral papillae clumps separated from one another at midline, papillae elongate, slender. Maxillary barbels present, separated from lateral lip margin.

Two pairs of dermal plates on lateral cheek margin between opercle and maxilla; anteriormost plate elongate and broad, positioned above anterolateral corner of lower lip above and posterior to maxilla, bearing odontodes on lateral edges; second posterior plate anterior to opercle, rectangular in shape with patch of larger odontodes on ventrolateral edge, smaller odontodes on lateral surface. Three or four small plates bearing odontodes in region between dorsal opercle margin and ventral pterotic margin.

Dorsal fin ii,7; first two rays segmented, unbranched, not thickened, without odontodes. Pectoral fin i,9; first ray segmented for half length, unbranched and thickened, anterior edge rugose, bearing odontodes; remaining rays branched and without odontodes. Pelvic fin i,5; first ray segmented, divided to base, greatly thickened, flattened; ventral surface bearing numerous large, blunt odontodes, arranged in 4–6 irregular rows along entire length. Anal fin ii,5; first two rays segmented, unbranched, not thickened, without odontodes, fin margin rounded. Adipose fin with well-ossified leading spine bearing odontodes, attached to trunk via short, thin membrane; three small anterior midline plates all bearing odontodes. Caudal fin i,14,i; three dorsal and three ventral platelike procurrent rays. Caudal fin deeply forked, lower lobe larger and extends slightly beyond upper lobe; tips of both lobes pointed.

Dermal plates on trunk consisting of three regularly arranged paired series of large plates located on posterior trunk, plus numerous small, isolated platelets arranged in somewhat irregular oblique bands located in region between dorsal and ventral plate series and extending anteriorly to vertical through anus. All plates bearing odontodes. Median plate series as continuation of dermal ossification of lateral-line canal; 14 (left) and 13 plates (right side); these plates distinguished from ossified lateralis canal segment in being distinctly larger, with expanded laminar ossification on dorsal and ventral margins of canal segment.

COLOR IN ALCOHOL: Dorsally pale brown grading to pale yellowish tan in irregular blotchy pattern; fins more uniform tan ventrally. Ventral surface uniformly pale.

DISTRIBUTION: Known only from the basin of Lago de Valencia, an endorrheic basin of northern Venezuela (fig. 4). The precise collection locality is unknown.

Lithogenes wahari, **new species**
Figures 6–8, table 1

HOLOTYPE: MBUCV-V-33738, 57.2 mm SL, ♀, Venezuela, Amazonas, Caño Päwä,

Fig. 6. *Lithogenes wahari*, male, preserved approximately 30 min after capture, showing coloration pattern against exposed Rio Cuao bedrock substratum.

approximately 30 minutes by foot upstream from its mouth into Río Cuao, approximately 30 minutes by boat downstream from Puerto Nuevo, 05°17.52′N, 67°19.74′W, coll. S. Schaefer, F. Provenzano, J.N. Baskin, SAS01-11, 8 March 2001.

PARATYPES: AMNH 233086, 42: 31.0–76.7 mm SL (12 ♀, 24 ♂), CAS 226002, 3: 40.5–56.9 mm SL (1 ♀, 2 ♂); FMNH 117747, 3: 45.3–66.4 mm SL (1 ♀, 2 ♂); MBUCV-V-29530, 35 (32, 3 cs): 34.0–78.3 mm SL, (17 ♀; 15 ♂), MCP 41962, 3: 41.4–54.6 mm SL (1 ♀, 2 ♂); USNM 392583, 3: 45.7–63.3 mm SL (1 ♀, 2 ♂) same data as holotype. MBUCV-V-27941, 62.1 mm. SL, ♂, Venezuela, Amazonas, raudal in alto Río Cuao, aprox. 05°30′N 67°0′W, coll. S. Zent, 9 November 1986.

DIAGNOSIS: Distinguished from all congeners by the absence of odontodes on the proximal portion of ventral surface of first

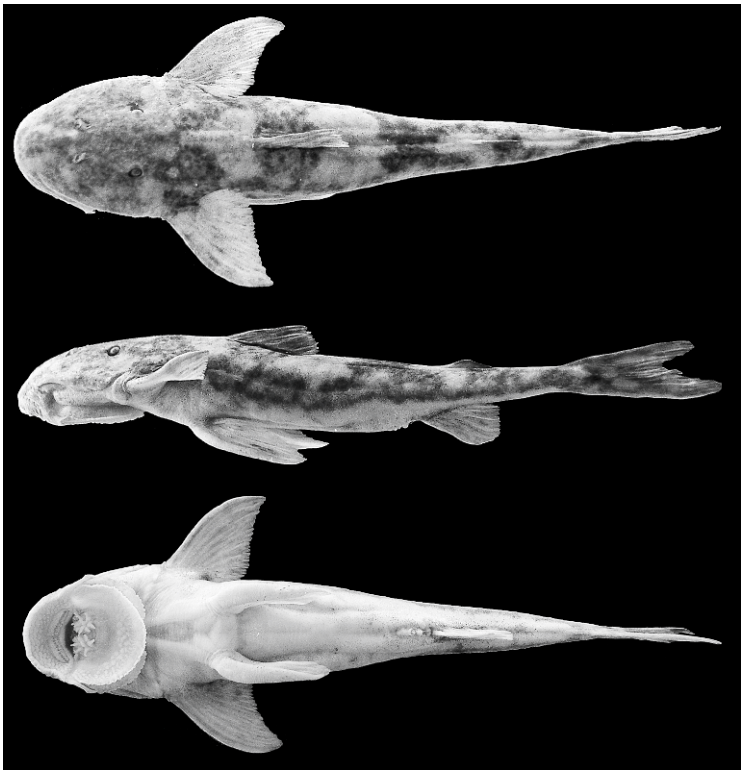

Fig. 7. *Lithogenes wahari*, holotype, MBUCV V-33738, 57.2 mm SL, female, Venezuela, Amazonas, Caño Päwä, Río Cuao basin.

pelvic-fin ray (vs. ventral pad covered with embedded odontodes along entire length, fig. 8); accessory premaxillary teeth absent; anal fin with intense pigment band along base and diffuse spot at midlength of fin rays (vs. pigment band at base absent, fin rays dusky, without distinct spot); adipose fin without ossified spine along anterior edge. Further distinguished from *L. villosus* by the presence of nine (vs. eight) branched pectoral-fin rays, absence of pigment band on snout lateral to nares; dermal plates on caudal peduncle small, irregular, plates of dorsal and ventral series not contacting plates of midline series (vs. plates large, regular in shape, dorsal and ventral series plates contacting those of midline series posteriorly). Further distinguished from *L. valencia* by the narrower, deeper head shape, head width 78% HL (vs. 80–95% HL), seven branched anal-fin rays (vs. five), 12 premaxillary teeth (vs. 25–28), tooth cusps asymmetrically bifid (vs. symmetrically bifid).

Description: Counts and measurements of holotype and paratypes given in table 1. Head and body moderately slender, not extremely depressed. Greatest head width (HW) at opercle, 18.8%–22.8% SL. Head shape bluntly triangular in dorsal view, snout gently rounded, margins tapered. Trunk elongate, slender, gently tapered posteriorly; greatest body width (BW) at pectoral-fin base, 23.4%–29.3% SL, greatest body depth (BD) at vertical through pelvic-fin origin, 15.6%–19.3% SL. Dorsal aspect of head gently convex in lateral view, dorsal margin of trunk straight from dorsal-fin origin to caudal fin. Ventral profile of head straight, abdomen between pectoral and anal-fin origins gently convex, trunk distinctly concave along anal-fin base, caudal peduncle straight. Trunk extremely slender in region posterior to adipose fin, least caudal peduncle depth 33.3%–45.5% BD. Caudal peduncle elongate, terete, becoming slender posteriorly. Anus

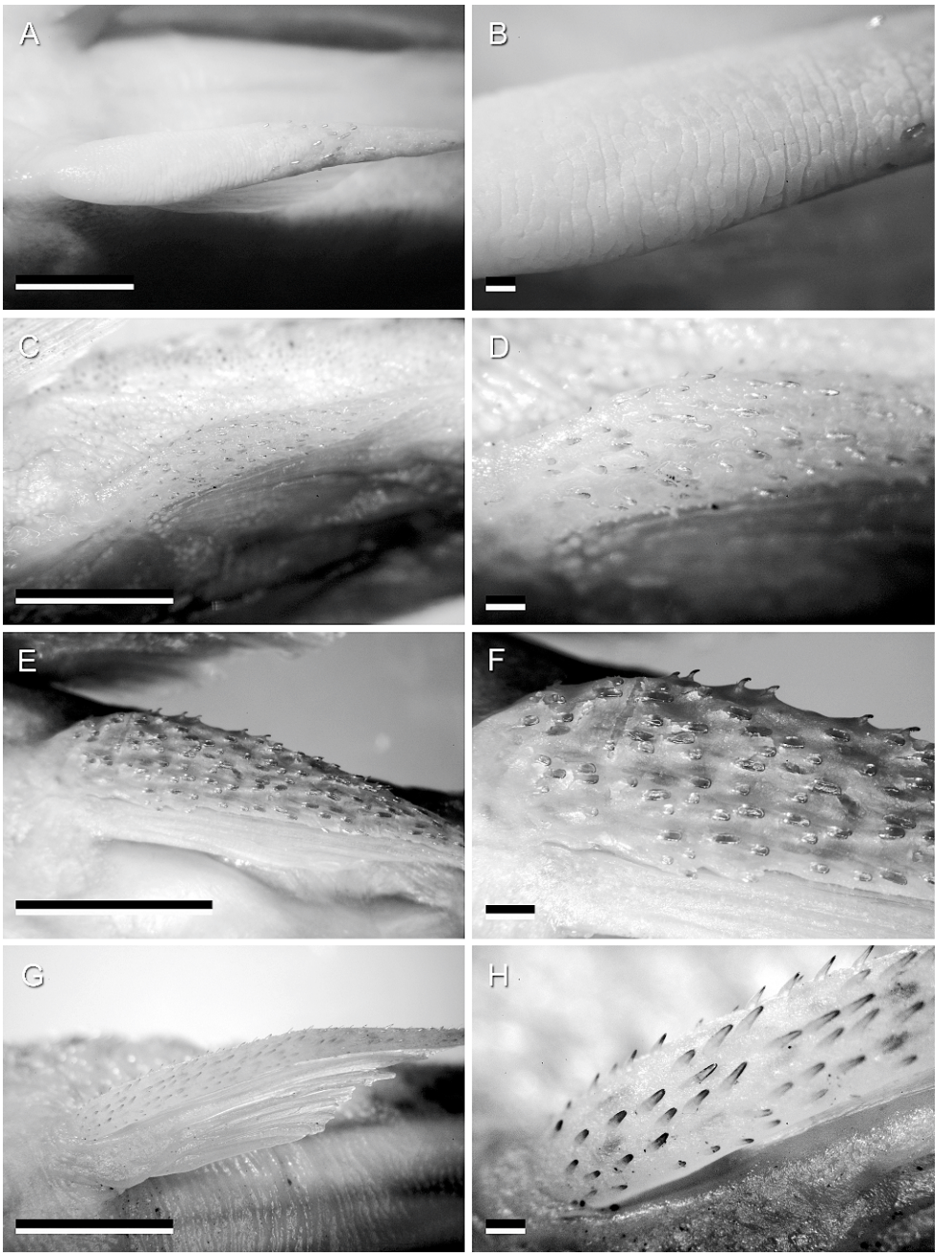

Fig. 8. Pelvic-fin pad, left side, ventral view. **A, B,** *Lithogenes wahari* AMNH 233086, female; **C, D,** *L. villosus* AUM 28152, female; **E, F,** *L. valencia* holotype, MBUCV V-30740, male; **G, H,** *Astroblepus* sp. MEPN 1599. Scale bar is 5 mm in A, C, E, G; 1 mm otherwise.

located midway between pelvic-fin origin and caudal-fin base, tubular. Urogenital papilla (see Body Size and Sexual Dimorphism, below) positioned immediately anterior to anal-fin origin.

Eyes moderately large, 7%–13% HL; posterior bony orbit margin positioned at vertical through opercle articulation with hyomandibula. Interorbit width broad, 35%–42% HW. Iris operculum absent. Nares ovoid, longer than wide, positioned midway between snout tip and posterior orbit margin; nares juxtaposed, separated by thin vertical skin flap, internaris width 15%–22% HW.

Premaxillary teeth 10–13 (12/13*) in single emergent row on each jaw element; asymmetrically bifid, cusps separated by V-shaped space, major (medial) cusp bluntly rounded, minor (lateral) cusp blunt to slightly pointed. Accessory premaxillary dentition absent. Dentary teeth 2–3 per jaw element; tooth and cusp shape bilobed and longer than the premaxillary, lobes of equal length and thickness. Replacement teeth as per emergent dentition, although cusps slightly more symmetric in size and shape.

Oral disk ovoid, wider posteriorly; ventral surface smooth immediately anterior to premaxilla, upper lip bearing large circular papilla arranged in transverse rows to anterior margin; a wide, non-papillate zone immediately anterior to premaxillae. The upper lip less deep than lower lip, anterior margin smooth and diverging laterally as a short maxillary barbel located at confluence of upper and lower lips. Lower lip surface irregular; elongated papillae located distally near margin, more dispersed robust papillae distributed throughout lower lip surface, these more separate from one another relative to those of upper lip. Posterior lip margin bilaminar, consisting of thick ventral layer, overlain by thinner smooth layer of flesh that extends posteriorly beyond margin of ventral papillose layer. Dorsal layer fimbriate along margin, not continuous along posterior lip margin and separated by gap equal in width to premaxilla length. Region of lower lip at dentary immediately posterior to emergent teeth bearing paired raised cluster of 18–24 villiform papillae (fig. 3C); papillae elongate, slender, with pointed tips; paired papillae clusters separated from one another at midline, intervening region smooth. Maxillary barbels present, separated from lateral lip margin.

Odontodes present on cranial bones of dorsum, dermal plates of lateral cheek margin and trunk, and first unbranched rays of pectoral, pelvic, and caudal fins, on cleithrum near pectoral fin origin, on unbranched rays of all paired and median fins except dorsal and anal fins; absent from branched fin rays of all fins except caudal fin, where present along four-fifths length of branched rays; odontodes present on procurrent caudal-fin rays. Smaller odontodes variously distributed on trunk, associated with dermal plates between caudal fin and region at vertical through dorsal fin origin.

Postotic laterosensory canal with pterotic branch (Schaefer and Aquino, 2000) present, skin-surface pore located on pterotic ventral process at vertical through or slightly posterior to gill aperture and posterior to origin of levator operculi muscle. Preoperculomandibular canal branching from temporal canal within pterotic, single pore located on ventral aspect of cheek at vertical through posterior orbit margin representing lateral branch of preoperculomandibular canal at its exit from preopercle bone. Antepreopercular canal segment of preoperculomandibular canal present as slender tubular ossified segment located anteroventral to canal exit from preopercle at posterior margin of second lateral cheek plate. Antepreopercular canal continuing anteriorly to terminate as skin-surface pore along ventrolateral margin of cheek. Temporal canal with posterodorsally directed short medial branch segment in frontal, its terminus a pore at frontal-pterotic junction. Infraorbital canal branching off within sphenotic, five or six paired infraorbital bones with expanded laminar ossification yielding platelike appearance, bearing complete infraorbital canal with five or six skin-surface pores. Supraorbital canal in frontal complete, terminating as canal within elongate nasal bone. Lateral line complete, continuous on trunk from pterotic to caudal-fin base.

Three to five pairs of dermal plates on lateral cheek margin between opercle and maxilla; first two anteriormost plates elongate,

rectangular; positioned above anterolateral corner of lower lip above and posterior to maxilla, bearing enlarged odontodes on lateral edges. Three or four small plates bearing odontodes in region between dorsal opercle margin and ventral pterotic margin.

Dorsal fin ii,6; first two rays segmented, thickened, bearing odontodes along anterior edge; second ray occasionally unbranched, first ray shorter, about half length of second ray; first dorsal fin spinelet absent. Fin margin straight. Pectoral fin i,9; first ray segmented for half length, unbranched and thickened, anterior edge rugose, bearing odontodes; remaining rays branched and without odontodes; fin emarginated; three radials, first rounded, second and third radials elongate, slender, distal margins expanded. Origin of pectoral fin about even with or slightly anterior to posterior edge of oral disc. Pectoral fin when depressed reaching to posterior third of length of first anal-fin ray. Pelvic fin i,5; first ray segmented, divided to base, greatly thickened, flattened dorsoventrally; flesh of ventral surface thickened, bearing numerous transverse ridges and without odontodes proximally (fig. 8A, B), remaining rays branched and without odontodes. Origin of pelvic fin at vertical through point midway between supraoccipital tip and dorsal-fin origin. Anal fin ii,6* or ii,6,i; first two rays segmented, unbranched without odontodes (except in mature males), last two segmented rays entirely separate, independent, and articulate on the same radial, seventh ray (when present) unbranched. Posterior anal-fin margin rounded, anterior fin margin concave. Anal fin when depressed reaching vertical through posterior third or slightly beyond adipose-fin base. Posterior edge of anal-fin base anterior to vertical through adipose-fin insertion. Adipose fin low, triangular, without well-ossified leading spine bearing odontodes except in larger males. Caudal fin i,14,i; three dorsal and five ventral procurrent rays, posteriormost procurrent rays elongate, odontodes on principal and procurrent rays. Caudal fin posterior margin deeply forked, upper and lower lobes equivalent in size and shape.

Dermal plates on trunk consisting of single regularly arranged paired series of plates along median lateral line caudally, plus few small, isolated platelets irregularly arranged above and below median series plates in region of caudal peduncle between dorsal and ventral procurrent rays. A few small, irregularly arranged and isolated platelets along dorsal and ventral midline immediately anterior to procurrent rays; these platelets variable in number and extent, 3–7 in dorsal series and 1–3 or none in ventral series. Plate series extending anteriorly to vertical through anus. Plates on head restricted to region of lateral snout between opercle and maxilla, above the infraorbital series of plates, small plates surrounding nares and along lateral margin of frontals. A few small isolated platelets on body in region between pterotic margin, lateral line, and dorsal-fin origin; plates otherwise absent on head and trunk. All plates bearing odontodes.

Coloration: Pigmentation generally consisting of dark brown melanophores on an underlying tan ground coloration dorsally, cream yellow ventrally (fig. 6). Dorsum of head overall dark brown, melanophores arranged as diffuse clusters yielding slight mottled appearance, with lighter underlying ground coloration prominent above opercle, between nares, and in form of thin V-shaped mark between nares and anterior snout margin. Ventral surface unpigmented, except for pectoral fins, genital papilla, and area surrounding anal fin. Melanophores on dorsum of trunk generally diffuse, concentrated as three broad saddles along base of dorsal fin, between dorsal and adipose fins, and through posterior half of adipose fin to caudal-fin base. Dark pigmentation tending toward indigo blue in bright sunlight prior to preservation. Lateral surface of trunk with 5–6 diffuse irregular blotches between pectoral-fin origin and caudal fin; melanophores becoming progressively more diffuse ventrally. Intense concentration of melanophores in form of narrow band along anal-fin base. Fins uniformly dusky, pigment concentrated along segmented fin rays, interradial membranes unpigmented. Caudal fin with concentration of melanophores at base and broad diffuse, irregular vertical band across fin rays; anal fin with broad pigment band across median portion of rays, pelvic fin with

pigment concentrated along length of first branched ray; dorsal fin with multiple irregular bands; pectoral fin with diffuse concentration of melanophores along fin rays.

BODY SIZE AND SEXUAL DIMORPHISM: Sexual dimorphism is here defined as those external morphological characteristics that allow an unambiguous determination of sex. Differences between males and females can be of two types, depending on the life stage of first appearance of the morphology. In the first type, sexual dimorphism is evident at hatching. In the second type, morphological differences between males and females do not become evident until individuals reach sexual maturity. Additionally, morphological differences between males and females can be permanent, that is, independent of developmental stage, season of the year, and reproductive condition of the gonads, such that sex can be determined without difficulty. In other cases, differences between males and females can be temporary because these morphologies appear only when gonads are developed, during a certain developmental phase, or a particular season of the year (as when reproductive activities occur). The specimens of *Lithogenes wahari* reported upon herein were captured in March, and because of their relative abundance, we are able to describe morphological differences that permit sex determination relatively easily. Morphological differences between sexes are observed in the head, anal fin, and urogenital papilla.

Males are larger than females on average (fig. 9). Average standard length for males (59.9 mm) is significantly larger than that for females (46.3; t = 3.314, Bonferroni-adjusted $P = 0.009$); the same relationship was observed for centroid size (males 29.5, females 24.1; t = 2.619, Bonferroni-adjusted $P = 0.038$). MANCOVA based on 11 variables describing aspects of shape in dorsal view (fig. 1A) plus body depth showed no significant difference in overall shape between sexes (Wilk's Lambda = 0.207, F = 2.791, df = 11, 8; $P = 0.078$). However, similar analysis of 12 variables describing aspects of shape in ventral view (fig. 1C) revealed significant sexual dimorphism overall (Wilk's Lambda = 0.049, F = 11.423, df = 12, 7; $P = 0.002$), with four measures responsible for the difference (snout width, anus to anal-fin origin, oral-disk length, and pectoral to pelvic-fin distance; fig. 10), all without an interaction with size, except for mouth width (F = 6.083, $P = 0.025$). In males the anus, genital papilla, and anal fin are positioned further caudad relative to the pelvic fin, and the pelvic fin is positioned more caudad relative to the pectoral fin (fig. 10). Females generally have a wider mouth than males at all sizes (fig. 10). Relative warps analysis of body shape revealed substantial differentiation between sexes. Separate principal components analyses of the partial warp scores on both dorsal and ventral unilateral landmark datasets yielded segregation of the sexes along the first relative warp axis (figs. 11, 12). The pattern of landmark deformations represented by the relative warps is consistent with the findings based on analysis of distance data in showing posterior displacement of the anus region relative to the pelvic fin in males and the narrowing of the space between anus and anal fin in females (fig. 10). Compared to aspects of ventral shape, the deformation implied by the first relative warp from the analysis of dorsal landmark data (fig. 12) is more subtle.

In both males and females, the region between the anus and anal-fin origin forms a depressed trough between the paired retractor ischii muscles of the midtrunk. The trough is shallower in males, which have hypertrophied paired retractor ischii muscles relative to females. In females, the region within the trough between the anus and anal-fin origin is developed as a deep, blind pocket formed by multiple skin folds surrounding a central aperture (fig. 13). A small genital papilla with acute tip and orifice with a small fleshy projection occupies a skin fold forming the posterior wall of the skin pocket; the anal-fin origin is positioned caudally and is separated from the genital pocket by a deep recess. In males, the region homologous with the genital pocket of females is developed as a large, oblate spherical papilla. The structure is conspicuous, projects well beyond the boundaries of the trough, and is positively allometric with respect to body size. The papilla tip is acutely pointed, darkly pigmented, and projects caudally beyond a vertical through the

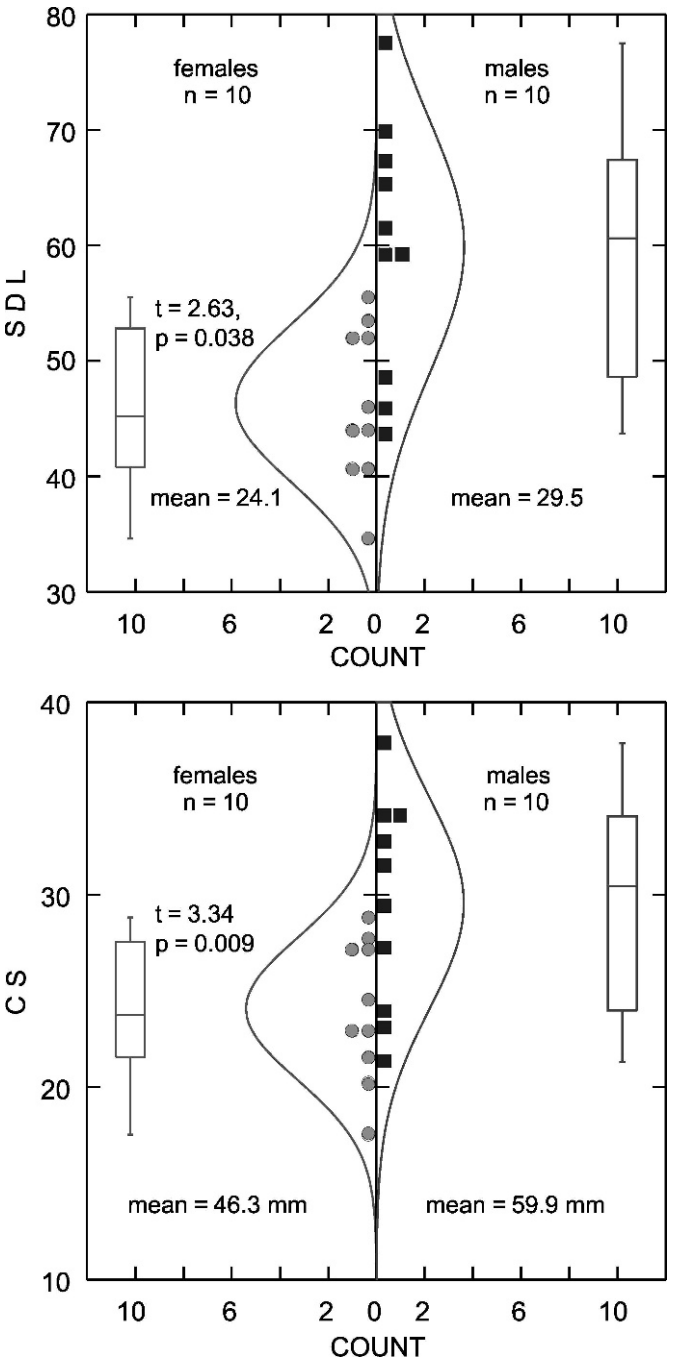

Fig. 9. Size dimorphism in *Lithogenes wahari*. Frequency distribution and descriptive statistics for standard length (top) and centroid size (bottom); rectangle depicts one standard deviation, horizontal line depicts mean, vertical line depicts range.

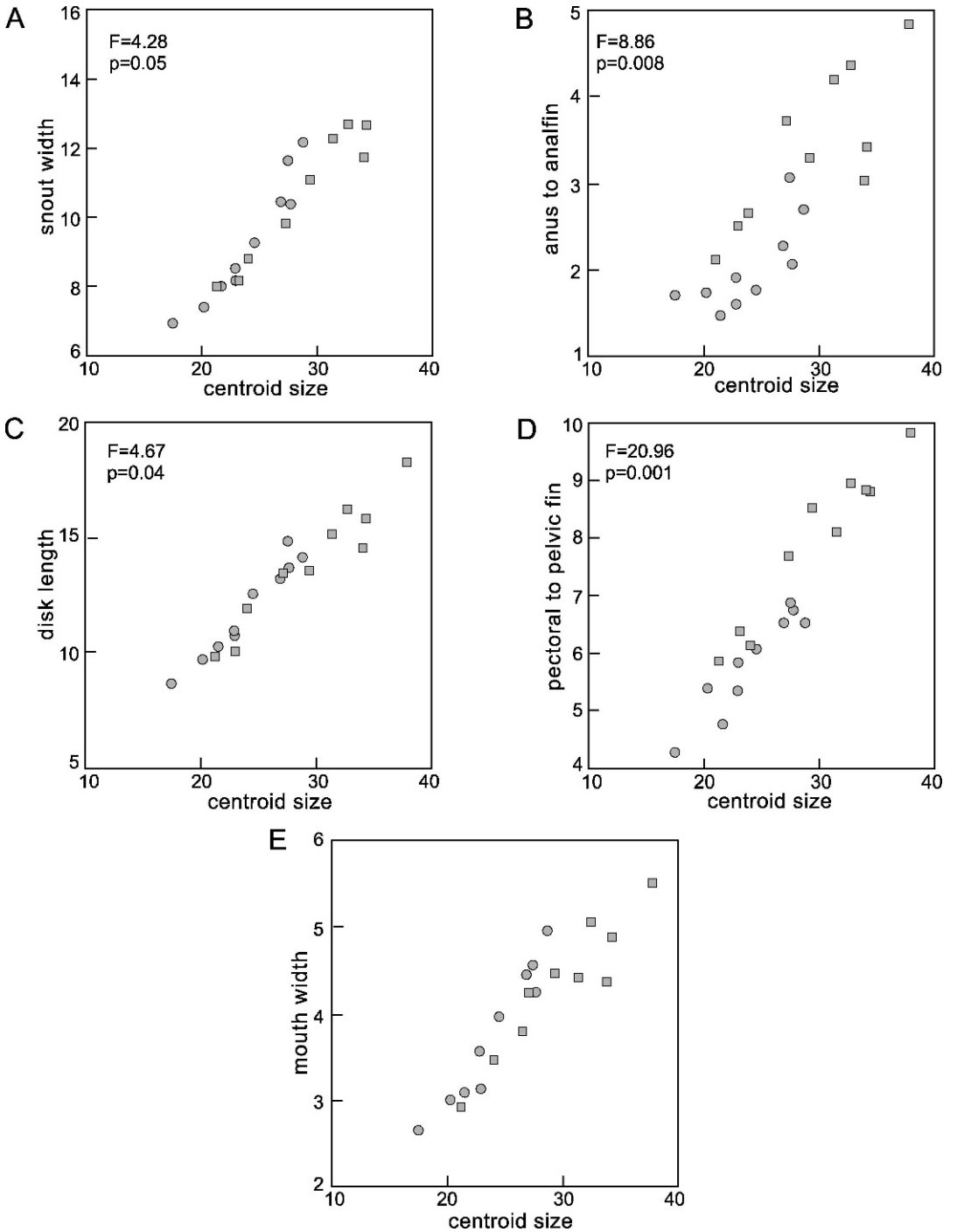

Fig. 10. Bivariate plots of morphometric features showing significant sexual dimorphism in *Lithogenes wahari*. Circles represent females, squares represent males. All variables except mouth width (E) have no significant interaction with centroid size.

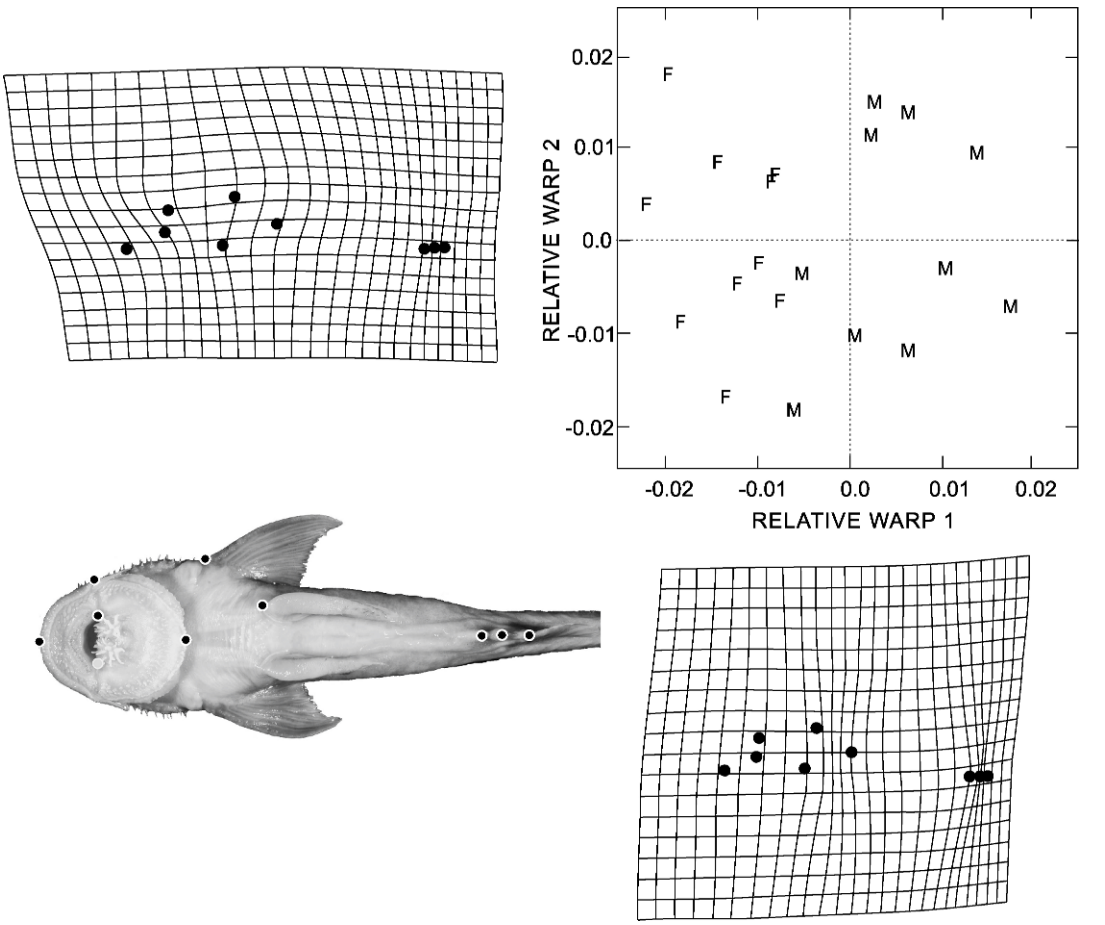

Fig. 11. Scatter-plot of scores from analysis of relative warps on ventral unilateral landmark coordinates for *Lithogenes wahari*. Pattern of shape contrasts described by the relative warp axes are depicted as two-dimensional grid deformations relative to landmark coordinates in ventral view (lower left). M, males; F, females.

anal-fin origin. The skin at the base of the anal fin is hypertrophied as a thickened fleshy pad along the anterior edge of the first anal-fin ray and separated from the expanded flesh surrounding the second ray by a deep channel (fig. 13). The genital papilla of males is separated from the fleshy pad forming the anterior margin of the first anal-fin ray, but the two structures closely abut one another. Dimorphism is present even in small-sized individuals (juveniles) that lack well-developed odontodes and skin papillae relative to larger, presumably mature individuals.

The skin on the dorsal and lateral surfaces of the head of males is adorned with small papillae, except for the area from the nostrils to the tip of the snout. Additionally, there are well developed odontodes on the dermal plates of the lateral head and snout. Females also possess odontodes and papillae in the same arrangement, but are not as extensively developed as in males. Males have thickened proximal portions of both the first and second anal-fin rays. These fin rays are curved slightly ventrad and have concave proximal margins, then become straight distally. A single mature specimen captured in November shares these distinctive morphological traits with male specimens captured in March, suggesting that the dimorphisms involving the urogenital

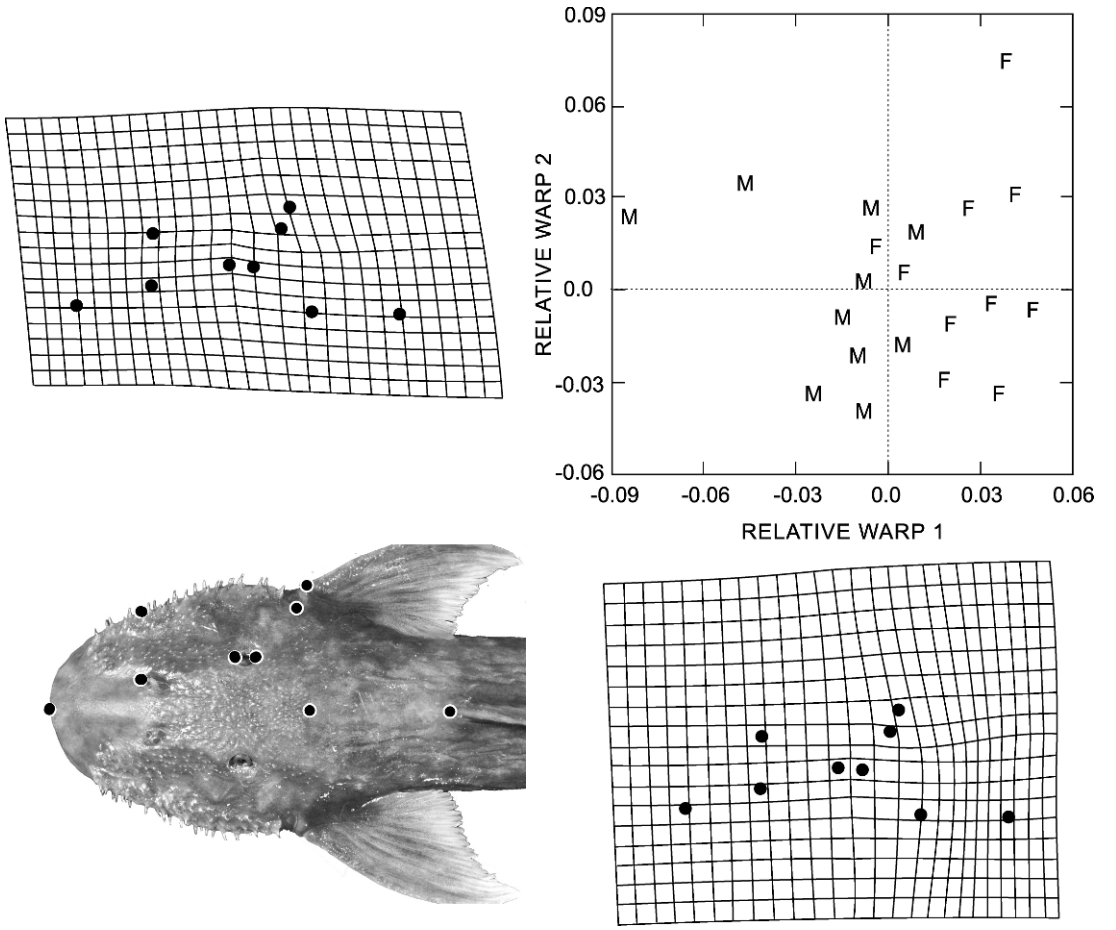

Fig. 12. Scatter-plot of scores from analysis of relative warps on dorsal unilateral landmark coordinates for *Lithogenes wahari*. Pattern of shape contrasts described by the relative warp axes are depicted as two-dimensional grid deformations relative to landmark coordinates in dorsal view (lower left). M, males; F, females.

papilla, anal fin, and head ornamentation represent permanent features, rather than seasonal or temporary conditions related solely to reproductive activity.

Digestive and Reproductive Anatomy: The anatomy of the digestive tract in *Lithogenes* differs from that of most other loricariids in lacking an extremely elongate, coiled intestine; however, they have a coiled intestine nonetheless. Instead, the morphology is somewhat intermediate between the typical loricariid gut, described in detail for the subfamily Hypoptopomatinae in Schaefer (1997), and that of the Astroblepidae, which possess a fairly simple, single-loop mid- and hind gut. In *Lithogenes*, the organs of the digestive system form a compact elongate spheroid mass within the body cavity between the pectoral girdle and anal fin. The digestive tract lies on either side of the urogenital organs, which occupy the midline immediately ventral to the vertebral column. The stomach and intestines form a series of loops around a central coil (fig. 14), which then passes to the hindgut and terminates at the anus. Pyloric cecae are absent.

Dorsal and ventral pharyngeal tooth plates covered with small conical, sharp teeth. Esophagus short, thin, and straight; connection with pharynx at the branchial apparatus clear, as it is its boundary with stomach.

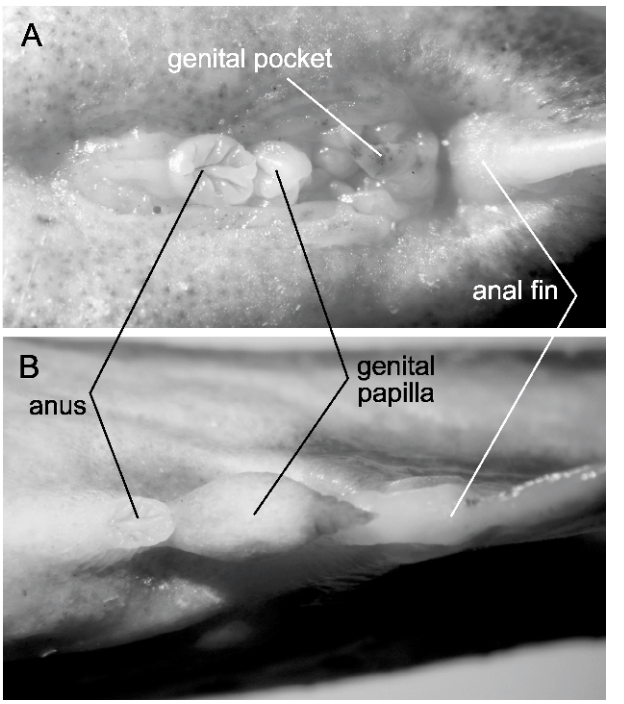

Fig. 13. Morphology of the urogenital region of *Lithogenes wahari* showing position of anus relative to genital papilla and anal-fin origin, ventral view, anterior toward left. **A,** female, 59.6 mm SL, region between anus and genital papilla forming deep pocket surrounded by complex skin folds; **B,** male, 63.2 mm SL.

Esophagus located superior to remainder of the digestive tract. Liver extensive, covering to a great extent the entire anterior region and most of the ventral surface of digestive organs.

The stomach is large diameter, thick walled, and elongate. Its diameter is at least twice that of the intestine. Its origin at the esophagus lies immediately ventral to the heart, from which point it passes to the right side of the body cavity, extends along the body wall to loop across the midline below the hindgut, and then turns back upon itself once again (fig. 14). There, the stomach narrows slightly at the pyloric transition to the intestine. The proximal intestine is large, its diameter equal to the greatest diameter of the stomach. It passes rostrally along the right side of the body cavity ventral to the stomach to the liver, where it turns dorsally and then caudally to loop back over the dorsum of the stomach along the right side of the body cavity. It then makes a loop across the midline dorsal to the loop formed by the stomach, and then passes rostrally along the left side of the body cavity. Anteriorly at a point posterior to the ventral lobe of the liver, the intestine forms a coil in the form of a quadruple loop with a reverse turn. The proximal portion of the coil turns clockwise (in dorsal perspective) to form two compact 360° loops, the second of which has a somewhat smaller radius and lies dorsal to the first. At the center of the coil on the midline, the intestine turns back on itself to reverse direction, with the resulting counterclockwise coiling distal portion forming another pair of loops continuing dorsally. The coil terminates at a transition to an expanded and elongate hindgut, which turns toward the left to pass caudally along the dorsum of the gut to its terminus at the anus.

Stomach contents of dissected specimens consist of fairly nondescript fibrous material that appears to be vegetable matter. No animal material was observed. Intestine contents consist of amorphous flocculent materials.

Gonads in one female and one male were observed in an advanced stage of maturity

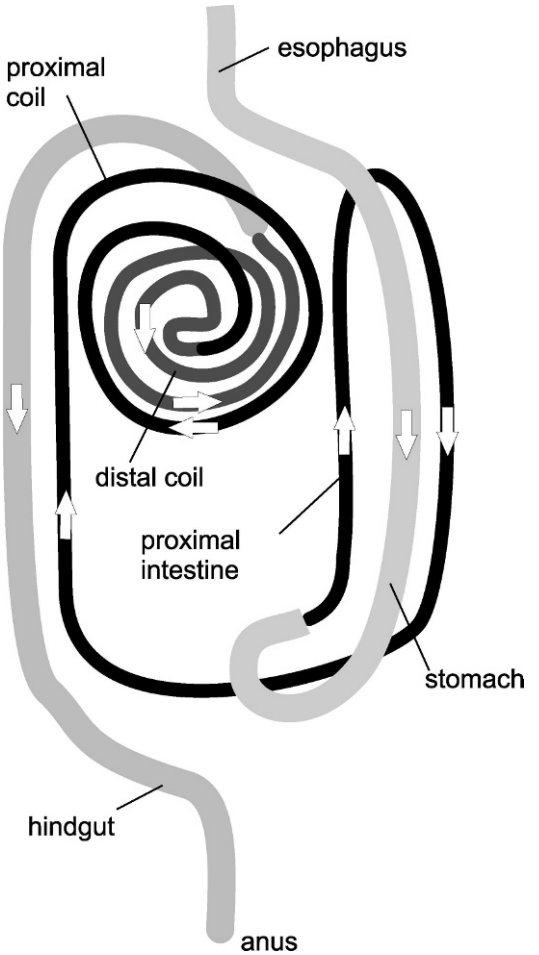

Fig. 14. Schematic representation of gut morphology and pattern of intestine coiling, *Lithogenes wahari*, ventral view, anterior toward top. Open arrows depict direction of passage.

(fig. 15). There is no evidence of hermaphroditism or sex reversal with size. Ovaries are paired structures above the digestive tract and liver and below the kidney, extend for approximately half of the visceral chamber, are cylinder shaped, and without any type of deformation, branching, or compartmentalization. Their anterior margin is rounded and their posterior margin is similar, attenuated only at the convergence with the urogenital papilla, where it seems both ovaries join (fig. 15A). No dermarkation between ovaries and oviducts was observed, and there is no structure that can be inferred as a receptacle for the urogenital papilla or sperm of the male. Ovaries are yellow due to the amount of vellum present in the mature ova, which are easily observed through the transparent ovarian walls (possibly due to extreme distension caused by the large size and advanced developmental stage of the eggs), the latter appearing granular and heterogeneous.

Counts and measurements of ova were made by direct observation through the transparent ovarian walls and without dissection. We observed a total of eight ova in the right lobe and seven in the left. Additionally we observed about 60 atresic ova, the largest ones creamy or yellow in color, the smallest ones almost transparent. The largest eggs were 3.2–3.5 mm in diameter; developing eggs ranged from 0.3 to 0.8 mm diameter. The near uniform size of developing ova, combined with the disparity in size between largest and smallest ova, suggest that egg maturity in this species is approximately synchronous. As with other members of the Loricariidae having similarly low fecundity, a high degree of parental care is suspected but unconfirmed at present. Low fecundity, restricted habitat requirements, and limited geographic distribution are characteristics of populations under potentially severe environmental risk. Consequent extinction seems to have occurred for *Lithogenes valencia*, a congeneric species that has not been observed in the field since the 1970s.

Testes of the two studied specimens are paired structures located dorsally above the digestive tract and liver, below the kidney, are ribbon shaped, without any type of branching or compartmentalization (fig. 15B). Their rostral margin terminates as a sharp tip; the caudal end is attenuated proximal to the urogenital papilla. There are no limits with the spermatic ducts, and it is remarkable that both testes appear to join before reaching the urogenital papilla. Testes are creamy white in coloration, homogeneous and fibrous in appearance.

DISTRIBUTION: Known only from the middle section of the Río Cuao, a clear-water tributary of the Río Sipapo of the Orinoco River basin of southwestern Venezuela (fig. 4).

HABITAT: Inhabitant of moderately high-gradient forest streams with clear water, swift

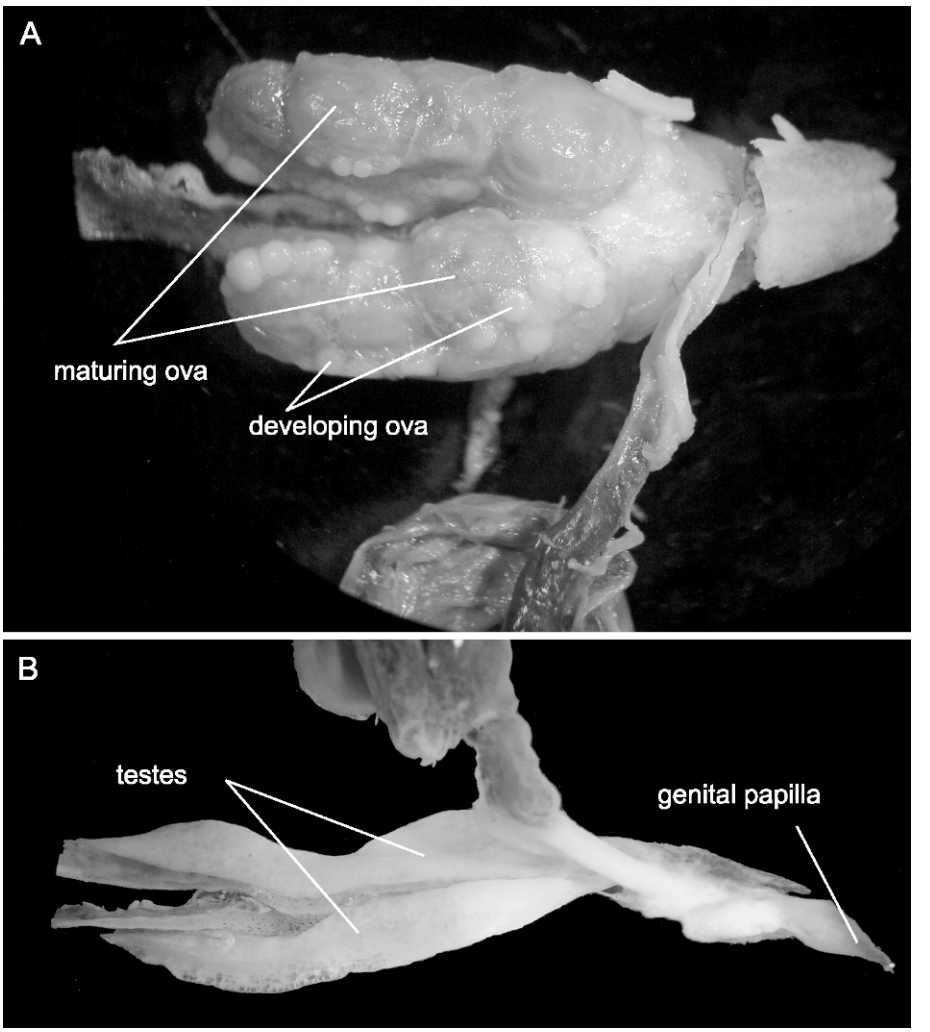

Fig. 15. Reproductive anatomy, *Lithogenes wahari*, dorsal view, anterior toward right. **A,** female; **B,** male.

current, and exposed bedrock substratum. The water color of the Río Cuao at the time of collection was clear to light green.

ETYMOLOGY: The specific name *wahari* is taken from the Piaroa name Rúa-Wahari, the god of the creation according to the Piaroa peoples, here treated as a noun in apposition to the generic name. According to legend, one day Rúa-Wahari created the first man from a mass of fish flesh at the place called Mariuek'a. Unattended for a period of time, the crabs came and consumed the flesh he had prepared. Rúa-Wahari fished once again and with each fish captured from the lake, he fashioned the eyes, the hair, the ears, the mouth, and the nose. In this way, Rúa-Wahari completed the first man and first woman.

COMPARATIVE ANATOMY

In this section, we present a comparative analysis of the anatomy of the lithogenine Loricariidae, with focus on the osteology and myology of *Lithogenes wahari* as a reference point for the comparisons. Material of *L. villosus* and *L. valencia* is limited and the

myology of these species is unknown, except for those features of the musculature visible through the skin. In order to facilitate comparisons and avoid repetition of anatomical description, the section is organized by body region in a general anteroposterior sequence, with treatment of the bones and connective tissues preceding that of the musculature for each successive anatomical system.

Cranium and Dermal Plates of the Cheek

In general aspect, the shape of the cranium of *L. wahari* is elongate and slender (fig. 16) relative to that of other lithogenines and other loricariids. This is a consequence of the narrow width of the frontal bones and a compact pterotic-supracleithrum lacking the expanded dorsolateral surface that covers the lateral opening of the swim bladder capsule typical of most Loricariidae.

Mesethmoid longer than wide, anterior portion broadly rounded, dorsal surface smooth and slightly convex; dorsolateral lamina slightly expanded at synchondral buttress with lateral ethmoid, dorsomedial lamina extending posteriorly over the buttress and sutured to anterior margin of frontals at transverse line through posterior margin of nasal capsule. Ventrally, articular condyle with premaxillae smoothly spherical, without ventral processes; midline shaft wide, without ventral lamina. Lateral lamina projecting anteriorly to form dorsal roof over mesethmoid condyle and separated from it by a distinct sulcus. Primordial ligament with a broad insertion along the lateral margin of the mesethmoid shaft.

Lateral ethmoids rectangular, wide anteriorly to accommodate an expanded nasal capsule. Anterolaterally with large condyle for articulation with palatine. Lateral margin concave, overlapped by frontal dorsally, exposed dorsal surface restricted to anterior third of bone. Unlike the condition in *L. wahari*, the lateral ethmoid of its congeners extends caudally to contribute to the orbit rim. Posteroventrally expanded at lateral junction with orbitosphenoid and forming deep concavity for origin of retractor tentaculi muscle. Ventral surface bearing tall, thin laminar ridge from below nasal capsule extending posteriorly onto ventral surface of orbitosphenoid. Nasal bones comprised of ossified laterosensory canal and moderate laminar components; positioned along mesial margin of nasal capsule.

Vomer broad across synchodral junction of mesethmoid and lateral ethmoids; anteriorly with short laminar extension underlapping mesethmoid, posteriorly with elongate, spike-shaped midline laminar process that interdigitates with anterior parasphenoid process. Frontals arrow shaped; broad at antorbital process, becoming narrow anteriorly toward midline suture with mesethmoid; overlapping the dorsal surface of lateral ethmoid.

Orbitosphenoids square in outline, laterally developed as process at junction with frontals and forming anterior margin of orbit. Ventral surface with laminar ridge, continuous with that of lateral ethmoids. Parasphenoid triangular, with slender elongate anterior shaft underlapping midline junction of orbitosphenoids, tapered posteriorly, sutured to basioccipital at midline, laterally to mesial margins of prootics.

Sphenotic with slender, triangular lateral process, forming deep dilatator fossa for origin of dilatator operculi muscle; anterior and posterior margins straight, medial margin with strong interdigitation with supraoccipital. Prootics with large lateral concave facet for articulation with dorsal process of hyomandibula; medial margin with indentation at ventral floor of the foramen for cranial exit of the trigeminofacial nerve. Ventral surface flat; truncus hyomandibularis branch of facial nerve exits via large foramen at anterolateral corner, ramus opercularis branch exits via smaller, more posterior foramen. Basioccipital rhomboidal, with large interdigitating suture with parasphenoid; its posterior margin V-shaped at contact with Weberian complex centra. Exoccipital trapezoidal; foramen for cranial exit of vagus nerve (X) located along posterior margin and anterior to ridge formed by transverse lamina of Weberian capsule; exit for glossopharyngeal nerve (IX) via large foramen located medial to vagus foramen near junction with basioccipital and Weberian complex centra.

Pterotic robust, its lateral surface pierced by numerous irregular foramina, ventral surface

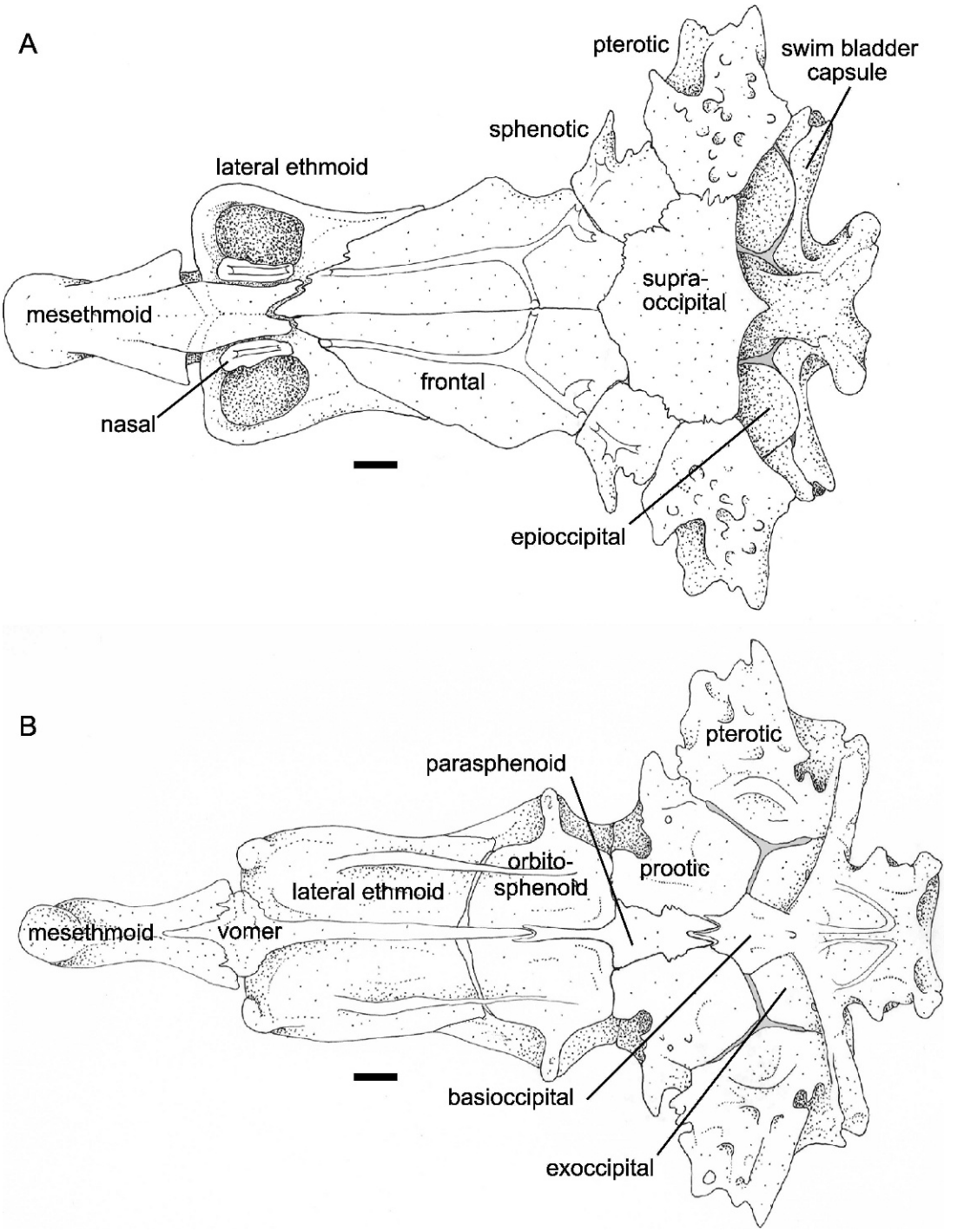

Fig. 16. Skull of *Lithogenes wahari*, AMNH 233086, anterior toward left. **A,** dorsal view; **B,** ventral view. Scale is 1 mm.

deeply concave. Anterolateral margin with deep recess, underlain by ventral lamina and forming large fossa for origin of levator operculi. Ventrally with deep aperture that receives dorsal process of cleithrum, pterotic aperture not open dorsally; posterior margin forming elevated ridge at junction with transverse lamina of Weberian capsule; anterior margin bearing strong interdigitating suture to hyomandibula.

Supraoccipital octagonal, with short anterior and posterior processes. Posterior face with short, shallow vertical lamina. Dorsoposterior limit of cranium formed by supraoccipital, epioccipital, and transverse lamina of Weberian capsule. Dorsal visceral nerve bundle exits from foramen at junction of supraoccipital and pterotic below posterodorsal supraoccipital ridge. Pterotic and transverse lamina of Weberian capsule forming restricted lateral opening of the swim bladder capsule, through which passes the trunk portion of the lateral-line nerve.

Cheek region comprised of thick dermal plates bearing enlarged unicuspid odontodes along lateral margin (fig. 17). Anteriorly, two large rectangular plates border the ventral margin of the fifth and sixth infraorbital plates; anterior aspect separated from the mesethmoid tip by large unplated region. Posterior cheek margin composed of 1–2 plates lateral to opercle and preopercle; cluster of 3–4 smaller rounded plates positioned dorsal to posteriormost cheek plate. Six plates in the infraorbital series; first two below eye with small laminar portions, fourth though sixth greatly expanded; all bearing laterosensory canal.

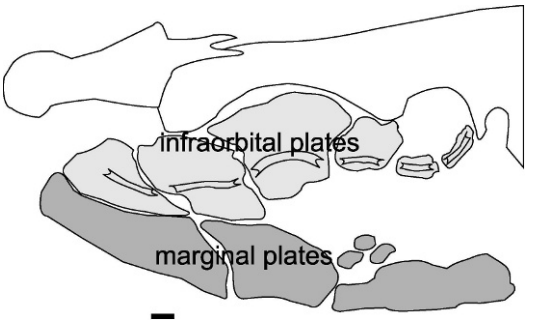

Fig. 17. Dermal plates of cheek region, *Lithogenes wahari*, lateral view, anterior toward left. Scale bar is 1 mm.

Mandibular Arch and Opercular Series

Hyomandibula rectangular, lateral surface with additional expanded shelf of bone lateral to principal lamina forming a deep recess extending from the dorsoposterior limit of the preopercle to the posterior limit of the quadrate (fig. 18). The lateral lamina extends laterally to the dermal cheek plates and subdivides fibers of the adductor mandibulae complex into dorsal and ventral bundles. Lateral lamina continuous posteriorly with vertical adductor crest, which is bifurcate dorsally, forming a cup-shaped lamina below the eye. The anterior bifurcation of the levator crest observed in *L. valencia* is absent in *L. wahari*. Posteromesial margin with strong interdigitating suture to pterotic. Mesial face of hyomandibula concave; large foramen for entrance of mandibular branch of the facial nerve positioned adjacent to pteroric suture and midway between sphenotic and opercular articular condyles, nerve branch exits hyomandibula on mesial face from foramen at ventral margin of bone anterior to opercle condyle.

Metapterygoid triangular, with thickened anterodorsal process that contacts the ventral lateral ethmoid ridge. Posteriorly, a small pointed process projects dorsally from the lateral surface. Among congeners, the posterodorsal metapterygoid process is shared between *L. wahari* and *L. villosus*, whereas *L. valencia* bears a homologous process on the hyomandibula, rather than on the metapterygoid. Preopercle lateral margin reflected dorsally, forming a thickened ridge supporting the enlarged dermal plates of the lateral cheek. Its anterior margin deeply concave, extending anteriorly along ventral margin of quadrate. Laterosensory canal lies mesial to lateral reflected ridge, bearing a single middle branch and pore in addition to input (dorsoposterior) and output (anteroventral) pores. Anteroventral laterosensory canal branch continues into thin canal-bearing plate lying ventral and mesial to the ventral margin of the lateral cheek plates. Quadrate slender, mandibular condyle blunt, dorsal margin syndesmotic with metapterygoid and synchondral posterior

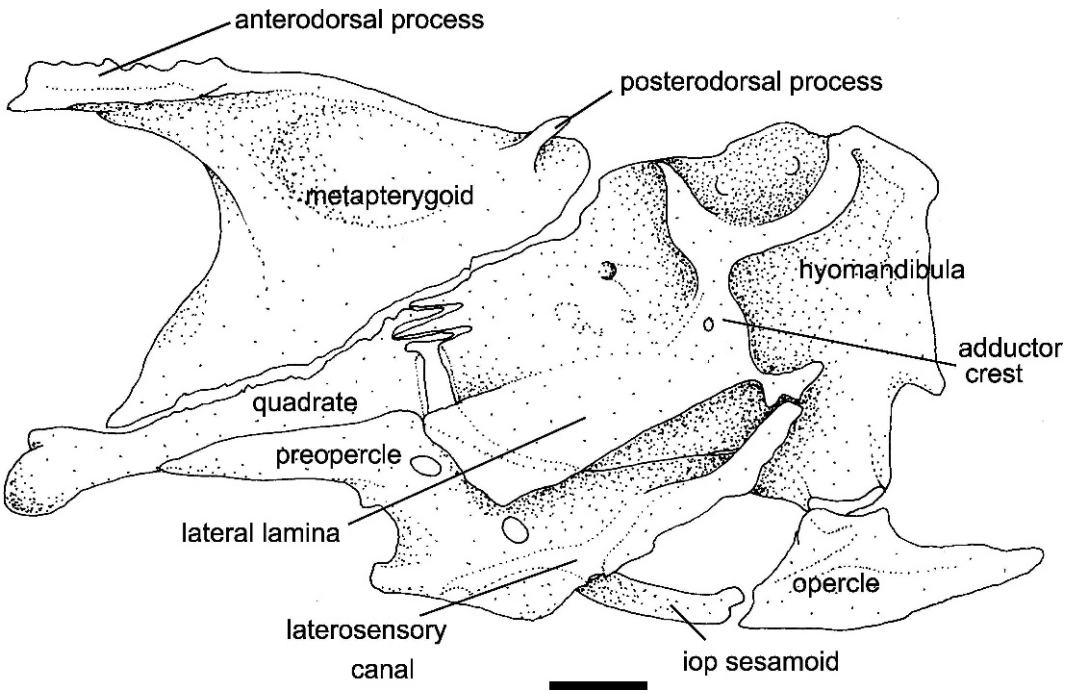

Fig. 18. Jaw suspensorium and opercle, *Lithogenes wahari*, left side, lateral view. Scale bar is 1 mm.

articulation via symplectic cartilage; strong interdigitating suture with hyomandibula posterodorsally. Opercle thin, anvil shaped, with broad dorsal articular facet. Its ventral margin convex, smooth; anteroventral corner attached to robust operculomandibular ligament bearing large cylindrical sesamoid bone. Interopercle absent.

Jaws and Teeth

Palatine short, robust; posterior (proximal) pair of processes for insertion of extensor palatine muscle subdivisions, and large concave condyle for articulation with lateral ethmoid. A short, thick ligament attaches the ventromedial extensor process to the vomer. Thick spike-shaped sesamoid bone closely adpressed to dorsolateral edge of palatine (fig. 19); its bony aspect extending from the palatomaxillary cartilage posteriorly to approach, but not reach, the palatine articular condyle with the lateral ethmoid, and continuous with a thick (unossified) ligament running caudally into the connective tissues associated with the dorsomesial rim of the fleshy nares.

Mandible comprised of dentary and compound anguloarticular bones. Dentary compressed laterally, cup narrow, elongate anteroposteriorly; three teeth in emergent row, 5–6 rows of subdermal replacement teeth arranged as per premaxilla. Coronoid process a slightly elevated crescentic ridge, concave posterolaterally; not developed as a robust coronoid horn as in other Loricariidae, coronoid horn absent in *L. valencia*. Anguloarticular short, compact; posterolateral process buttresses with corresponding process of dentary, and both articulate via connective tissue with reflected flange of metapterygoid. Maxilla sickle-shaped with angular anterior margin and gently concave posterior margin. Articular surface a large concave notch; posterodorsal corner developed as a rounded terminal cartilage. Palatomaxillary ligament very short, connects dorsomedial process of maxilla to dorsolateral surface of palatine articular cartilage (fig. 19). Medial surface of maxilla developed into an expanded lamina. A single broad, thick, fibrous fan-shaped mesethmomaxillary ligament attaches the mesial lamina to the mesethmoid lateral margin

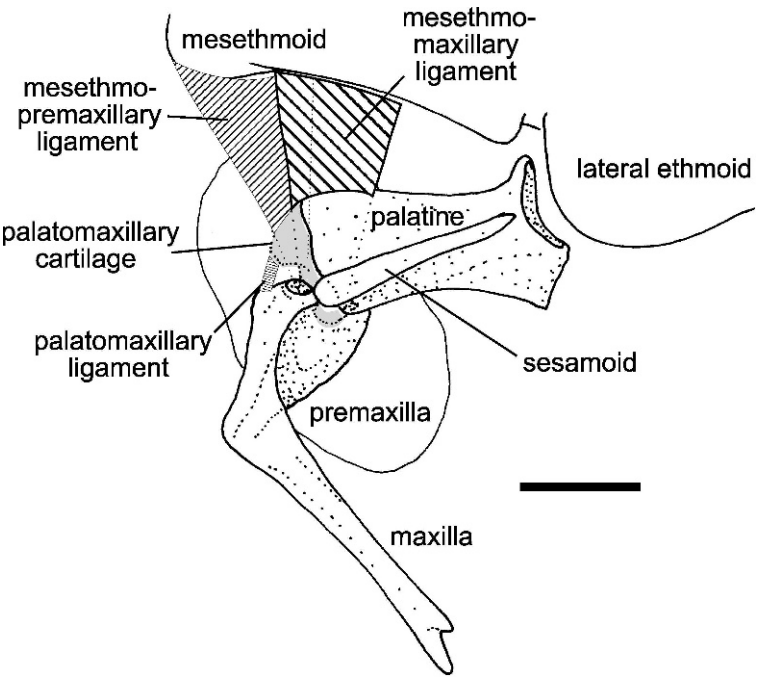

Fig. 19. Schematic illustration of the arthrology of the premaxilla and maxilla, dorsolateral view, anterior toward left. Scale is 1 mm.

(fig. 19). This ligament has a broad origin along the mesethmoid and overlaps the dorsal mesethmopremaxillary ligament. A thick, short ligament attaches the posterior surface of the maxillary lamina to the fibrous connective tissues of the palatopremaxillary cartilage.

Premaxilla rectangular, cup shaped; morphology similar to that typical of Loricariidae. Dorsal surface convex, smooth, with central shallow sulcus; ventral surface produced as deep cup enclosing a single row of emergent teeth plus 5–6 rows of subdermal replacement teeth, subdermal rows arranged in anterior to posterior sequence of progressive degree of tooth development. Accessory teeth absent (fig. 20). Posteroventral surface with concave laminar shelf bearing narrow sulcus for insertion of the retractor premaxillae muscle. Mesial surface convex, with ventral sulcus and posterior tuberosity associated with extensive mesethmopremaxillary articular cartilage. Twelve teeth in emergent row, tooth cusps asymmetrically bifid, cusps bluntly rounded.

Premaxillae articulate with the skull via two arthroses: a mesial articulation via the mesethmoid condyle (ethmopremaxillary joint), and a dorsolateral articulation with the anterior end of the palatine (palatopremaxillary joint). The mesethmopremaxillary ligament (fig. 19) originates from the dorsolateral lamina of the mesethmoid and inserts on a dorsal premaxilla condyle. An unpaired transverse ligament connects the two premaxillae across the anterior midline. The flesh of the upper lip immediately above the premaxilla and maxilla is developed as a thick sheet of stiff connective tissue forming a cap or shield, crescent shaped anteriorly at the midline, bearing thin strands of connective tissue between the crescent portion and the premaxilla. Connecting tissue strands forming two pairs: the lateral pair thin, elongate, connecting to the premaxilla at the anterolateral corner of the dorsal surface of bone; the posteromesial pair broader, short, attaching posterior edge of the crescent-shaped cap to the dorsomedial aspect of the premaxilla. A dorsolateral extension of the sheet forms an articular cap to the head of the maxilla.

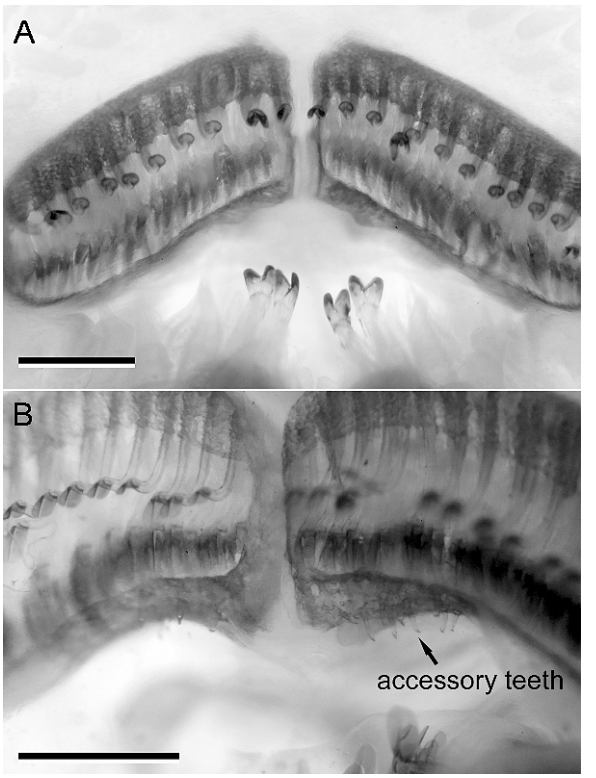

Fig. 20. Cleared and stained specimens showing premaxilla and distal tips of dentary teeth, ventral view, anterior toward top. **A,** *Lithogenes wahari*, AMNH 233086, showing absence of premaxillary accessory teeth. **B,** *L. valencia*, CAS 28361, showing accessory teeth present (arrow). Scale is 1 mm.

The mesethmopremaxillary cartilage is an unpaired spherical mass on the ventral spherical surface of mesethmoid at the midline, forming an articular surface between the mesethmoid and premaxilla. The cartilage occupies the space between the dorsally projecting condyles of the paired premaxillae. Primordial ligament a broad sheet of connective tissue occupying the medial palatine region with attachment between the mesethmoid, premaxilla, and dentary. Ligament extended anteriorly along the lateral margin of the mesethmoid shaft, passes posteriorly below the lateral ethmoid lateral to the palatine and connects to the premaxilla and maxilla.

Muscles of the Cheek

Levator tentaculi (fig. 21) rectangular, straplike on lateral surface of cheek. Origin elongate, from lateral margin of frontal, beginning at corner of antorbital process, along entire frontal concave margin and continuing along lateral margin of lateral ethmoid lateral to naris, to point where the margin curves medial. Free lateral edges of muscle straight. Insertion on posterodorsal margin of maxilla shaft and dorsal surface of concavity formed by expanded mesial head of maxilla at palatine articulation.

Adductor mandibulae (fig. 21) with four subdivisions. Three distinct muscles occupy the lateral cheek anterior to the orbit; the largest (A2dorsal) lies dorsal to the horizontal lamina of hyomandibula, and two smaller bundles (A2ventral α, β) lie ventral to the horizontal lamina. A2dorsal comprises the major muscle component of cheek between the suspensorium and the mandible. It has a broad origin from anterolateral surface of the horizontal and anterior margin of the vertical

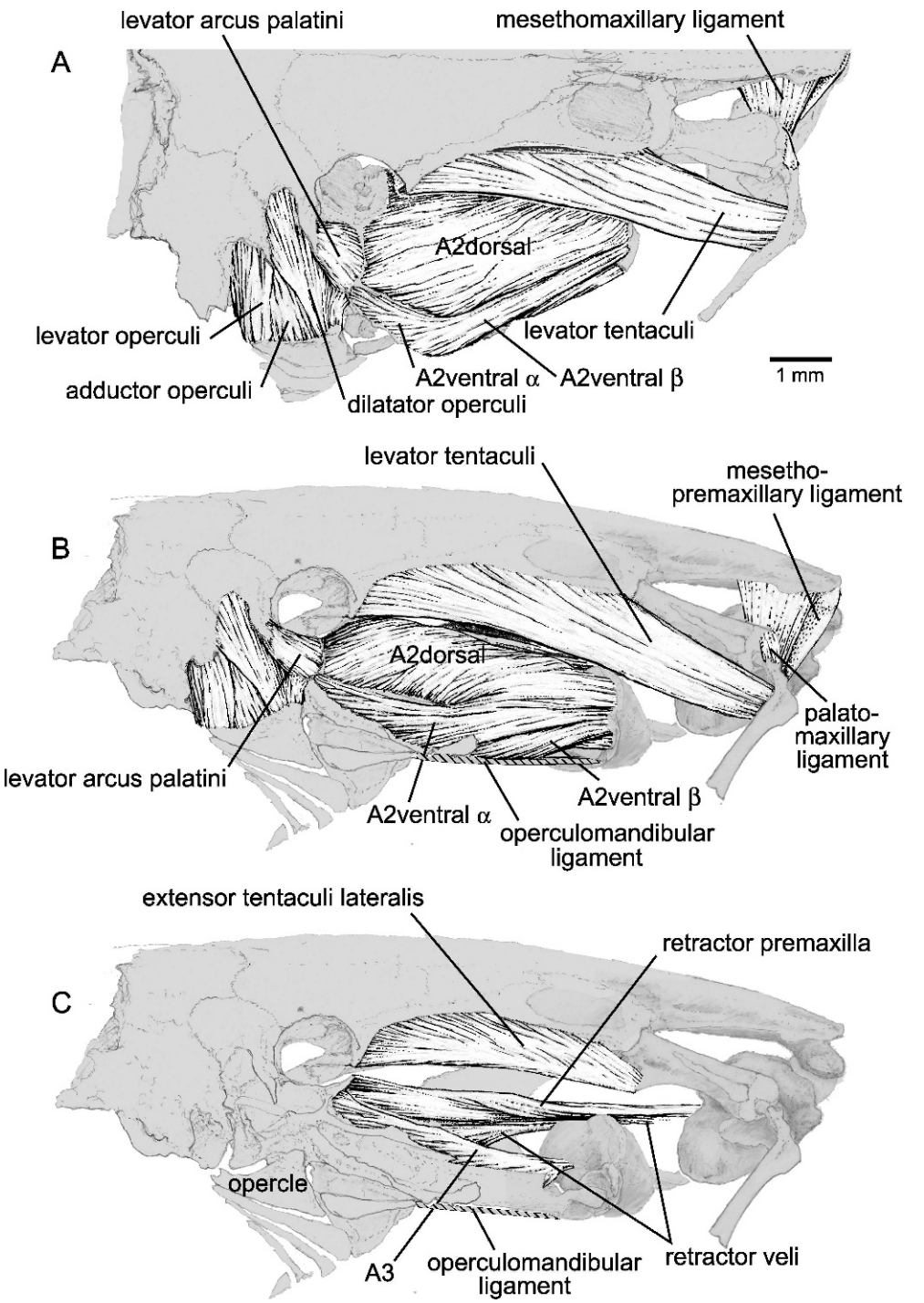

Fig. 21. Cranial muscles of cheek, *Lithogenes wahari*, anterior toward right. **A,** dorsal view; **B,** lateral view; **C,** lateral view of underlying musculature after removal of levator tentaculi and superficial adductor complex. Drawings by Ian Hart.

hyomandibular crests; its insertion is on the posterior lamina of the dentary at the coronoid process. A2ventral α is more narrow and less robust, occupying the large, deep fossa of the hyomandibula formed by the horizontal lateral lamina and the recurved ventral margin of the preopercle. Its origin is along the posterior margin of the fossa and it inserts on the dorsolateral process of the anguloarticular at a point dorsal to the articulation with the quadrate condyle. A2ventral β comprises a thin, narrow strip of muscle (perhaps merely a ventral subdivision of A2ventral α) running parallel and adjacent to the operculomandibular ligament. It originates from the laterally reflected dorsolateral margin of the preopercle and it inserts on the dorsolateral anguloarticular process ventral to the insertion of A2ventral α. The fourth adductor division (A3) is a large muscle lying mesial to A2dorsal and ventral to the retractor premaxillae muscle. It has a broad crescent-shaped origin from anterior lateral lamina of hyomandibula anterior to orbit; it inserts on the dentary at the coronoid process ventral and anterior to fibers of the A2dorsal.

Retractor premaxillae (fig. 21C) an elongate, thick muscle of the dorsal cheek, lying mesial to A2dorsal and immediately underneath ramus lateralis nerve branch to levator tentaculi and maxilla. Origin from the lateral hyomandibula lamina and anterior face of the vertical adductor crest anterior to the orbit; its insertion via a thick, narrow tendon onto a small sulcus of the premaxilla at midline of posteroventral surface of tooth cup.

The retractor veli (*retractor palatini* of Howes, 1983; Schaefer and Lauder, 1986) is present in *Lithogenes* (fig. 21C) as a small, thin slip of muscle with an elongate tendinous insertion onto tissues of the lateral corner of the oral valve. The tendinous portion is approximately 50% the length of the entire muscle system. The muscle lies deep beneath both the A2dorsal division and partially beneath the mesial A3 division of the adductor mandibulae. The muscle originates from the subocular shelf and vertical crest components of the hyomandibula. Anteriorly, its tendinous component passes beneath the retractor premaxilla.

Extensor tentaculi lateralis (fig. 21C) is an elongate, straplike muscle on the dorsolateral margin of the cheek below the lateral margin of the cranium. Its origin is extremely elongate, involving the entire lateral margin of the lateral ethmoid and frontal. Its deep-lying fibers originate from the concave antorbital fossa of the lateral ethmoid formed bony ridges and a ventral continuation of the antorbital process; its insertion is via a thin tendon onto the posterolateral palatine process.

Extensor tentaculi medialis is comparatively smaller. Its origin is from the ventral surface of the orbitosphenoid and lateral ethmoid and it occupies a shallow groove formed by a ventral lateral ethmoid ridge laterally and a midline shaft of the parasphenoid mesially. Its insertion is via a thick tendon onto the posterodorsal palatine process beneath the nasal capsule.

Levator arcus palatini is a broad, fan shaped muscle lying superficially on the lateral cheek between the dilatator and levator operculi muscles and the origin of A3. Its origin is from the postorbital process of the sphenotic below the orbit; its insertion is broad, along the posterior margin of the vertical hyomandibular adductor crest and the dorsal margin of the posterodorsal adductor crest.

Dilatator operculi, a long conical muscle bundle, is positioned superficially on the dorsoposterior aspect of the cheek between the levator operculi and levator arcus palatini muscles. Its origin is from within dilatator fossa, a deep concavity along the lateral skull margin at the junction of the sphenotic and pterotic-supracleithrum. Its insertion is via a tendon onto the anterodorsal process of the opercle. Dorsally, fibers of the dilatator operculi merge with those of the levator arcus palatini at the origin point on the ventral tip of the sphenotic postorbital process.

Levator operculi, a broad, rectangular thin muscle, is positioned superficially on the posterior aspect of the cheek behind the dilatator operculi. Its origin is from a large pterotic fossa and its insertion is along the entire dorsal margin of the opercle.

Adductor operculi is broad and flat, lying mesial to the levator operculi. Its origin is from the pterotic and it inserts on the dorsomedial margin of the opercle, mesial to the insertion of the levator operculi.

The adductor arcus palatini is not visible externally, as it lies mesial to the proximal mass of the adductor musculature. The muscle comprises a broad, wide thin sheet between the cranium and suspensorium. Its origin is from the ventral surface of the orbitospenoid and lateral ethmoid (between ventral crest and parasphenoid at midline) and it inserts on the mesial surface of the hyomandibula and metapterygoid.

Adductor hyomandibulae a thin sheet. Its origin from the ventrolateral prootic margin and it inserts onto the mesial surface of the hyomandibula ventral to its cranial articulation.

Muscles of the Lip and Hyoid

Intermandibularis posterior with separate ventral (labialis) and dorsal (dentalis) subdivisions (fig. 22). Ventral subdivision thick, straplike; origin from ventrolateral margin of posterohyal and anterohyal; insertion deep on underside of lip just posterior and slightly lateral to ventral mandibular papilla mass. Dorsal subdivision a rectangular muscle, lying above lateral segment of labialis division; origin from anterior face of posterohyal, insertion via thick, broad tendon onto posteroventral surface dentary tooth cup.

Intermandibularis anterior a small paired bundle on deep underside of lower lip. Paired bundles share common origin at antimere on midline, fibers diverge laterally. Short anterior bundle runs anterolaterally to insert on lip tissues posterior to papillae mass. Longer posterior bundle runs posterolaterally to insert on lower lip posterior to the lip insertion of the intermandibularis posterior labialis division. The intermandibularis anterior muscles are not associated with the dentary bone or the intermandibular cartilage, except via connective tissue at the ventral midline.

Hyohyoideus inferioris bifurcate, distinct sections separate laterally at anterohyal insertion at the level of the first branchiostegal ray. The anterior and posterior divisions share a common origin at the midline, positioned posteroventral to the midline union of the hypohyals. Anterior section large, straplike; fibers running laterally dorsal to intermandibularis posterior and inserting broadly along the ventral surface of the anterohyal. Posterior section shorter, less broad; fibers laterally separating from anterior section at posterior margin of anterohyal, insertion along posteroventral edge of anterohyal just anterior to branchiostegal rays.

Hyohyoideus abductores short, thick; lying between posteromedial edge of first branchiostegal ray and cleithrum; fibers oriented perpendicular to longitudinal body axis, lying ventral to sternohyoideus. Unlike other catfishes, the muscle originates from cleithrum, rather than to parurohyal or anterohyal. Hyohyoideus adductores broad, thin; positioned across distal ends of the branchiostegal rays.

Sternohyoideus broad, short; contralateral bundles completely separate from antimere at midline. The muscle lies dorsal to the hyohyoideus inferioris and anterior to the insertion of the protractor ischii bundle onto the parurohyal at the midline. Fibers are directed posteriorly and nearly parallel with longitudinal body axis between the parurohyal posterior margin and anterior edge of cleithrum.

Branchial Arches

The hyobranchial skeleton (fig. 23) is comprised of the bones and connective tissues of the hyoid arch plus branchiocranium. In lithogenines, like other loricariids, the hyoid arch is coupled to the mandibular arch via the intermandibular cartilage and associated connective tissues.

Hypohyal a single ossification, rectangular in outline and relatively compressed. Connected to anterohyal along its lateral margin via thick synchondrosis dorsally and direct synarthrosis ventrally. Anterior surface with ventral concavity and medial blunt process forming an articular surface with the intermandibular cartilage. Posterior surface with thickened transverse shelf forming ventral margin of a recess into which projects the anterolateral process of the parurohyal.

Parurohyal broad and wing shaped, its anterolateral margins nearly straight and extended, lateral wings narrow, its posterior margin sigmoid. Anterior paired cornua project into ventral recess of hypoyhals. Posterior aspect of bone extremely short, without

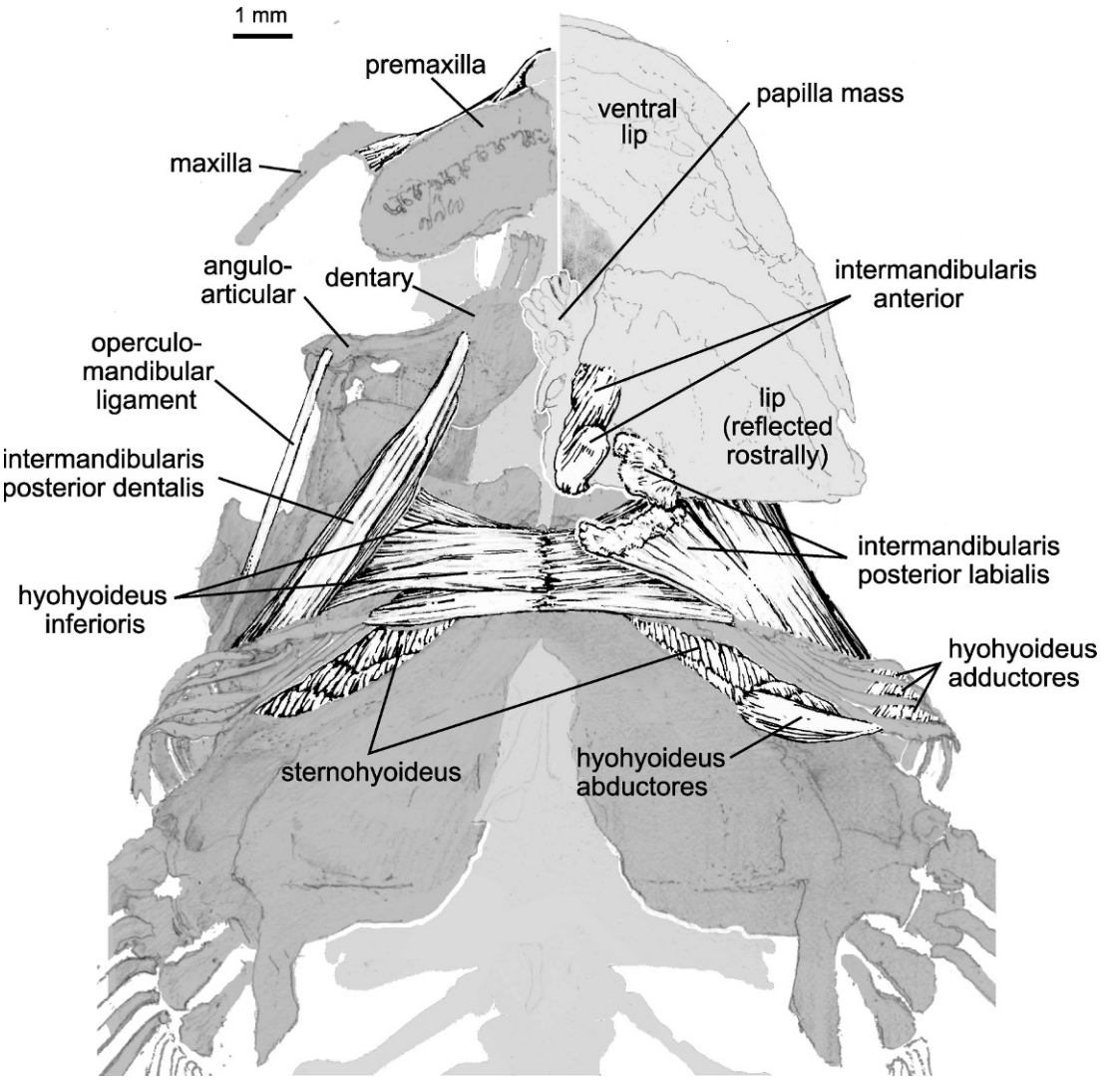

Fig. 22. Hyoid musculature, *Lithogenes wahari*, ventral view, anterior toward top. Schematic representation after removal of lips and the intermandibularis labialis from right side, lower lip of left side reflected ventrorostrally and separated from the intermandibularis labialis insertion. Drawing by Ian Hart.

laminar midline component, not projecting caudally beyond joint between antero- and posterohyals, forming concave recess dorsal to anterior tip of cleithra at midline. Dorsal surface with pair of small processes surrounding basibranchial cartilage; hyobranchial foramen small. Lateral wings narrow proximally and becoming slightly wider distally, tip sharply pointed.

Anterohyal robust, rectangular, with greatly expanded anterior and posteroventral laminae. Connected to posterohyal laterally via elongate synchondrosis dorsally and posteriorly, and via direct synarthrosis along anterolateral margin. Anterior lamina expanded, with convex anterior margin and large foramen. Posterior lamina triangular, greatly expanded laterally along margin with posterohyal.

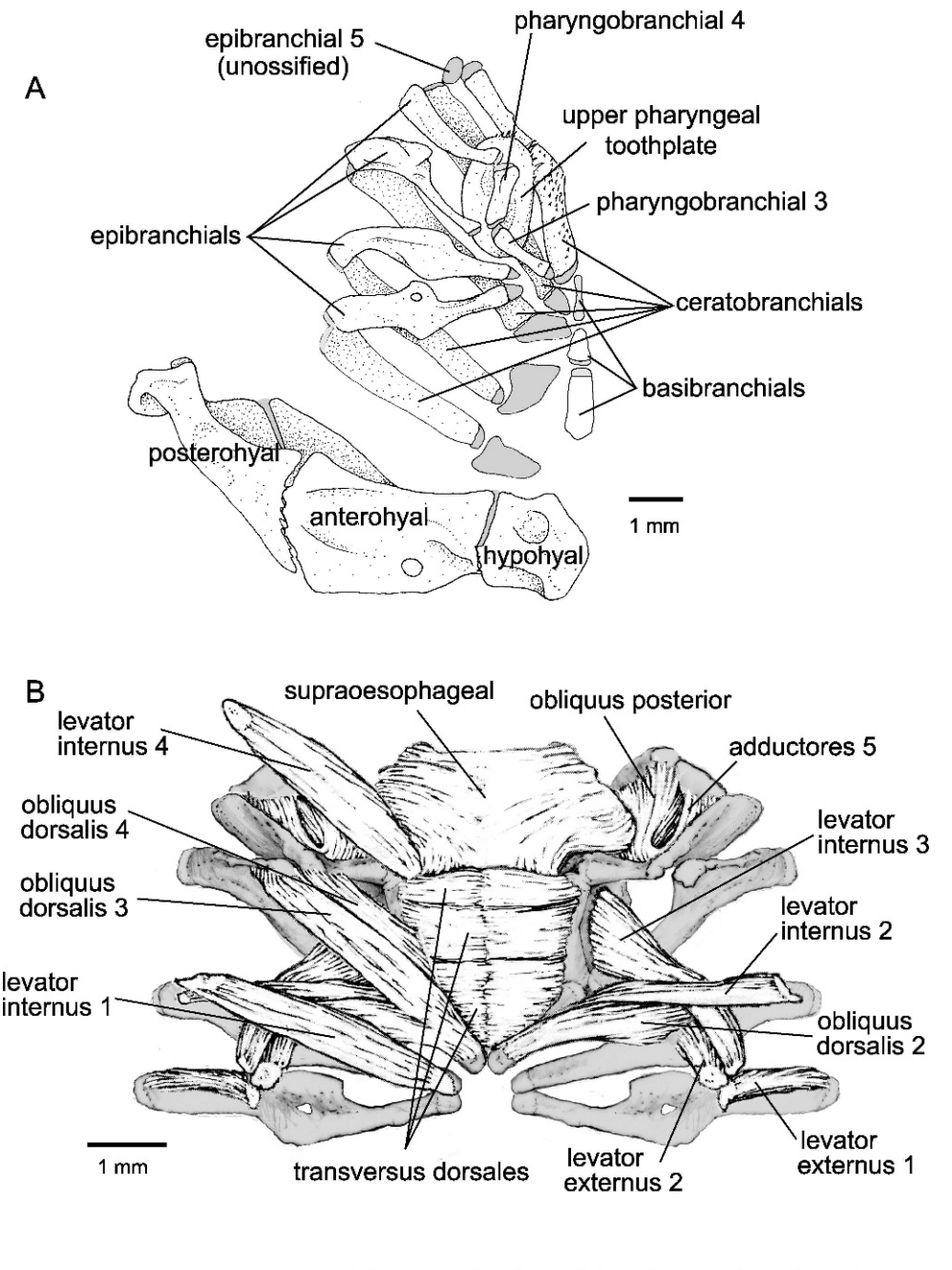

Fig. 23. Hyobranchial skeleton, right side (**A**) and musculature (**B**) of *Lithogenes wahari*, dorsal view, anterior toward bottom. Dorsal levator muscles removed from left side to reveal deeper musculature. Scale is 1 mm. Drawing B by Ian Hart.

Posterohyal triangular in outline, with greatly expanded anterior and posteroventral laminae. Dorsolateral edge of anterior lamina thickened at ligamentous connection to interhyal. Posteroventral surface expanded; along with lateral aspect of anterohyal, forming an enlarged surface for origin of hyohyoideus inferioris. Interhyal present as a small discoid ossification tightly adpressed to the mesial surface of the hyomandibula at dorsal margin with preopercle. Attached via thick ligament to thickened dorsoposterior ridge of posterohyal.

Branchial skeleton with five paired ceratobranchials and four paired epibranchials. Ceratobranchials (except for fifth) relatively straight, bar shaped; first ceratobranchial without ossified accessory lamina. Proximal ends of third and fourth ceratobranchials expanded. Fifth ceratobranchial with expanded posterodorsal lamina bearing extensive minute unicuspid teeth on dorsal (oral) surface. Cartilage cap on distal tip of fourth ceratobranchial bearing an enlarged, bulb-shaped posteromedial process that supports the connective tissues and cartilage at the distal end of the fifth ceratobrancial. Epibranchials slender proximally, variously shaped and expanded distally. First two epibranchials with triangular anterior process and expanded posterior lamina; third epibranchial triangular, with large blunt dorsal process for insertion of third obliquus dorsalis. Fourth epibranchial crescent shaped, with slender proximal shaft and expanded posterodorsally. Filamentous laminar fleshy gill rakers arranged across oral surfaces of all branchial arches, including the anterior margin of the fifth ceratobranchial; an additional row of rakers lie anterior to the first arch and are borne by the tissues spanning the hyoid and branchial arches, extend from the anterior process of the first epibranchial, span the epiceratobranchial joint, merging into the epithelium of the first ceratobranchial near its proximal end. Two pairs of pharyngobranchials. Element corresponding to third pharyngobranchial slender, rod shaped, ends slightly expanded; free in connective tissues, its proximal (medial) end associated with proximal cartilage tips of epibranchials 1–2, distal (lateral) end associated with cartilaginous junction of third epibranchial and fourth pharyngobranchial above dorsomedial margin of upper pharyngeal tooth plate. Element corresponding to fourth pharyngobranchial robust, compressed; its posterior end greatly expanded; oriented vertically, its ventral margin tightly associated (not free) with groove on dorsal margin of upper pharyngeal tooth plate. Upper pharyngeal toothplate robust, discoid, compressed dorsoventrally, dorsal surface concave, ventral surface convex, rounded. Oral surface bearing extensive field of minute unicuspid teeth.

First (anteriormost) two pairs of hyobranchial elements separate from cartilagenous tips of corresponding ceratobranchials, unossified. Three unpaired basibranchials. First (anteriormost) ossified, robust; trapezoidal in shape with blunt, expanded anterior margin; positioned between first and second hyobranchials. Second ossified, triangular, much smaller than first, with blunt anterior margin and rounded posterior apex. Third unossified, rod shaped, positioned between proximal cartilage of fourth ceratobranchial. Small spherical cartilage anterior to first basibranchial, positioned dorsal to parurohyal and attached to posterodorsal margin of anterohyal elements.

Levator externi (1–2, fig. 23) on dorsum of first two epibranchials. Both muscles originate from the prootic ventral surface posterior to origin of adductor hyomandibulae. The first levator inserts on the dorsal surface of the distal shaft of the first epibranchial, its orientation oblique, fibers directed anterolaterally relative to longitudinal axis; the second levator inserts on the anterodorsal margin of the second epibranchial mesially, its orientation nearly vertical (perpendicular to ventral surface skull).

Levator interni (1–4) involve the four epibranchials. Levator internus 1 elongate, its origin from prootic lateroposterior to levator externus origin and insertion on proximal tip of second epibranchial. Levator internus 2 shorter, origin from prootic and insertion on pharyngobranchial 3; its orientation from posterior to anterior, fibers cross dorsal to those of levator internus 3. Levator internus 3 longer, its origin from prootic at site of levator externus origin, insertion on upper

pharyngeal toothplate; orientation from anterior to posterior, fibers cross ventral to those of levator internus 2. Levator internus 4 elongate, fibers oriented posterolateral to anteromedial (parallel to orientation of levator internus 1); its origin from pterotic and insertion on posterodorsal buttress/process of the upper pharyngeal toothplate.

Obliqui dorsales (2–4, fig. 23) on the second through fourth epibranchials. Following Springer and Johnson (2004: 10), the name designation used here derives from the epibranchial on which the particular muscle inserts/originates. Obliquus dorsalis 2 origin from posterodorsal expanded lamina of epibranchial 2 to posteromedial margin of the shaft of pharyngobranchial 3. Contra Springer and Johnson (2004: 9), who regard the obliquus dorsalis 2 present only in osteoglossomorphs among pre-acanthomorphs, this muscle in *Lithogenes* is not considered a homolog of their Pb3-Eb2 muscle, which they state as being present only in Pomatomidae among acanthomorphs and not present *Diplomystes*. The occurrence of this muscle among siluriforms is unknown at present. Until confirmed otherwise, the proposal of nonhomology of this muscle in *Lithogenes* with an obliquus dorsalis seems less parsimonious than a novel, arbitrary designation. Obliquus dorsalis 3 origin from a dorsal uncinate process of the third epibranchial and insertion on posteromesial shaft of pharyngobranchial 3. Obliquus dorsalis 4 origin from the curved anterodorsal margin of epibranchial 4 to pharyngobranchial 4.

Transversus dorsales subdivided into three sections that span the dorsal midline between the pharyngobranchials and the upper pharyngeal toothplate. The anteriormost bundle spans the midline between the paired pharyngobranchial 3 and is confluent laterally with fibers of the obliquus dorsalis, the middle bundle spans the midline between pharyngobranchial 4, and the caudal bundle spans the midline between the upper pharyngeal toothplates; fibers merge with those of the supraesophageal musculature posteriorly.

Obliquus posterior thick, robust; its origin from the posterolateral portion of ceratobranchial 5 and laterally from the cartilagenous nodule of epibranchial 5, insertion on epibranchial 4. Medially, its fibers converge on a raphe with the supraesophageal laterally. Adductores 5 a separate distinct muscle bundle between posterior margin epibranchial 4 and the connective tissue surrounding the unossified epibranchial 5.

Transversus ventralis (not shown) comprises two separate muscle sheets spanning the midline between ceratobranchials. Transversus ventralis 4 between ceratobranchial 4; transversus ventralis 5 across ventral surface of ceratobranchial 5. Recti ventrales (1–3) and obliqui ventrales (1–3) between ceratobranchials and corresponding unossified hypobranchials; fibers not interdistinguishable. Rectus communis extends along ventral midline between ceratobranchials 3–4 and ventromedial lamina of parurohyal. Pharygoclavicularis externus and internus from ceratobranchials 4 and 5 to cleithrum.

Axial Skeleton and Caudal Fin

Thirty-five vertebrae including five vertebrate incorporated into the Weberian apparatus and fused to the skull, and the compound ural complex are regarded as single elements, respectively. Vertebra 6 with extensive direct sutural contact with the Weberian complex anteriorly, its dorsal midline lamina short, sutured to posterior aspect of Weberian complex below supraoccipital ventral lamina. Ventrally, vertebra 6 with transverse parapophysis developed into an enlarged club-shaped process bearing a posterior concavity that receives the proximal ventral aspect of the enlarged rib. Vertebra 7 concave dorsally with short dorsal lamina developed as a pocket that receives a proximal process of the first dorsal-fin pterygiophore; anteroventrally with enlarged zygapophysis that contacts vertebra 6. Vertebrae 7 through 16 bearing robust ribs, each having direct articulation with a lateral concavity of the centrum, located just caudad to the posterior ventral zygapophysis of the preceding vertebra. Ribs becoming progressively more slender and shorter posteriorly; rib on vertebra 17 connected ligamentously to the centrum. Vertebra 9–15 bifid dorsally, their dorsolateral lamina triangular in shape, becoming progressively smaller posteriorly. Vertebra 6–16 without hemal arch. Vertebra

20–22 with bifid ventral hemapophyses that straddle the proximal ends of the second through fourth anal-fin pterygiophores. Neural spines developed as expanded dorsal midline lamina on all vertebra posterior to and including vertebra 14; hemal spines developed as expanded ventral midline lamina on all vertebrae posterior to and including vertebra 26, becoming progressively elongated posteriorly to ural complex.

Caudal fin i,7-7,i and with three dorsal and five ventral procurrent rays. Caudal skeleton with hypurals, uroneural, and parhypural fused into a single complex (fig. 24A). Epural a separate element. Anterior margin of dorsal complex with thickened buttress along posterior margin of preceding neural spine. Hypurapophysis an elongate, tall laminar shelf extending from the centrum articulation anteriorly to the posterior hypural notch that demarks the primitively separate second and third hypurals.

Interradialis muscle a set of discrete bundles of fibers associated with the superficial fascia covering the proximal branched fin rays and inserting on the more distal portions of the rays. Muscle fibers converge on the median 3–4 fin rays at the midline. The flexor dorsalis superior and flexor ventralis superior muscles occupy the superficial layers of the caudal fin and are each subdivided distally. The flexor bundles each insert on the proximal heads of the branched fin rays via thin, broad tendon sheets. The flexor dorsalis inferior and flexor ventralis inferior are separate narrow bundles that lie beneath the superior bundles. Hypochordal longitudinalis an elongate and thin superficial muscle whose fibers diverge from the hypaxialis and pass rostrodorsally within the thin superficial connective tissue fascia to insert via a narrow thin tendon on the proximal shaft of the upper unbranched finrays. Supracarinalis and infracarinalis muscle bundles occupy the dorsal and ventral margins of the musculature, respectively, and each inserts on the proximal head of the largest posteriormost procurrent fin rays.

Pectoral Fin

Pectoral fin I,9; branched rays supported by a large discoid primary radial and two large club-shaped secondary distal radials (fig. 25). Primary radial with large concave articular surface with the corresponding convex articular condyle of the cleithrum. Posteriorly, the radial bears a process that projects within a recess formed by the bilateral halves of the pectoral spine and a posteromedial convexity that articulates with a large, thick cartilage block that spans the distal articular surfaces of the radials. Secondary radials robust, narrow, and more slender proximally at their cleithral articulation, becoming greatly expanded distally. Primary radial supporting the spine and first two branched rays, secondary radials supporting branched rays 3–4 and 5–9, respectively. The first unbranched ray (pectoral-fin "spine") is enlarged, thickened; solid proximally and the lepidotrichia becoming progressively more disconsolidated, the ray more segmented distally such that its distal third is quite flexible. Large odontodes evenly distributed along the entire length on both the dorsal and ventral surfaces of the lateral half of the fin ray; all branched rays without odontodes. Cleithrum with broad concave vertical lamina and single, bluntly rounded dorsal articular process. Horizontal lamina margin bearing a large, blunt process. Horizontal lamina broad, thin; its anterior margin bearing a short, blunt process.

Coracoid quadripartite, with robust relatively short posterior process. Horizontal lamina short, blunt; forming ventromedial margin of arrector ventralis foramen and not reaching medially to midline. Laterally bearing a robust convex condyle for articulation with discoid primary radial. Anterolaterally projecting as a narrow coracoid arrector bridge meeting a corresponding posterior strut of the cleithrum and together forming the ventrolateral margin of the arrector ventralis foramen. Posterolateral strut of mesocoracoid arch (fig. 25C) with sulcus that receives the proximal heads of the secondary distal radial elements.

Protractor pectoralis (fig. 25A) large, thick muscle band between ventral skull and cleithrum. Origin is from ventral surface of pterotic-supracleithrum along ridge formed by anterior margin of the bone boundary at hyomandibula suture, insertion is along anterior vertical lamina of cleithrum. Arrector

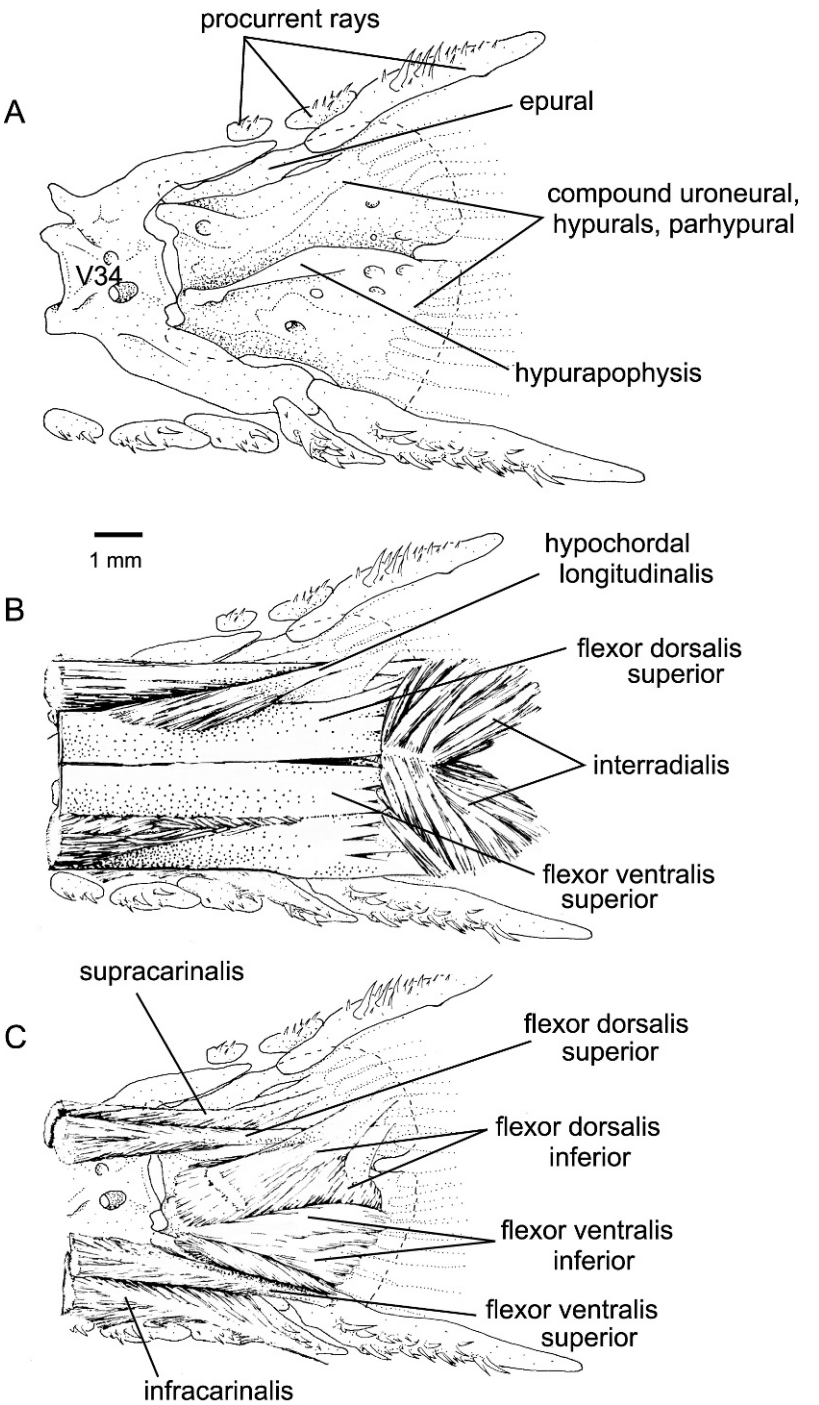

Fig. 24. Caudal fin skeleton (**A**) and musculature (**B, C**) of *Lithogenes wahari*, left side, anterior toward left. Superficial muscles removed to shown deeper musculature in C. Scale is 1 mm. Drawings by Ian Hart.

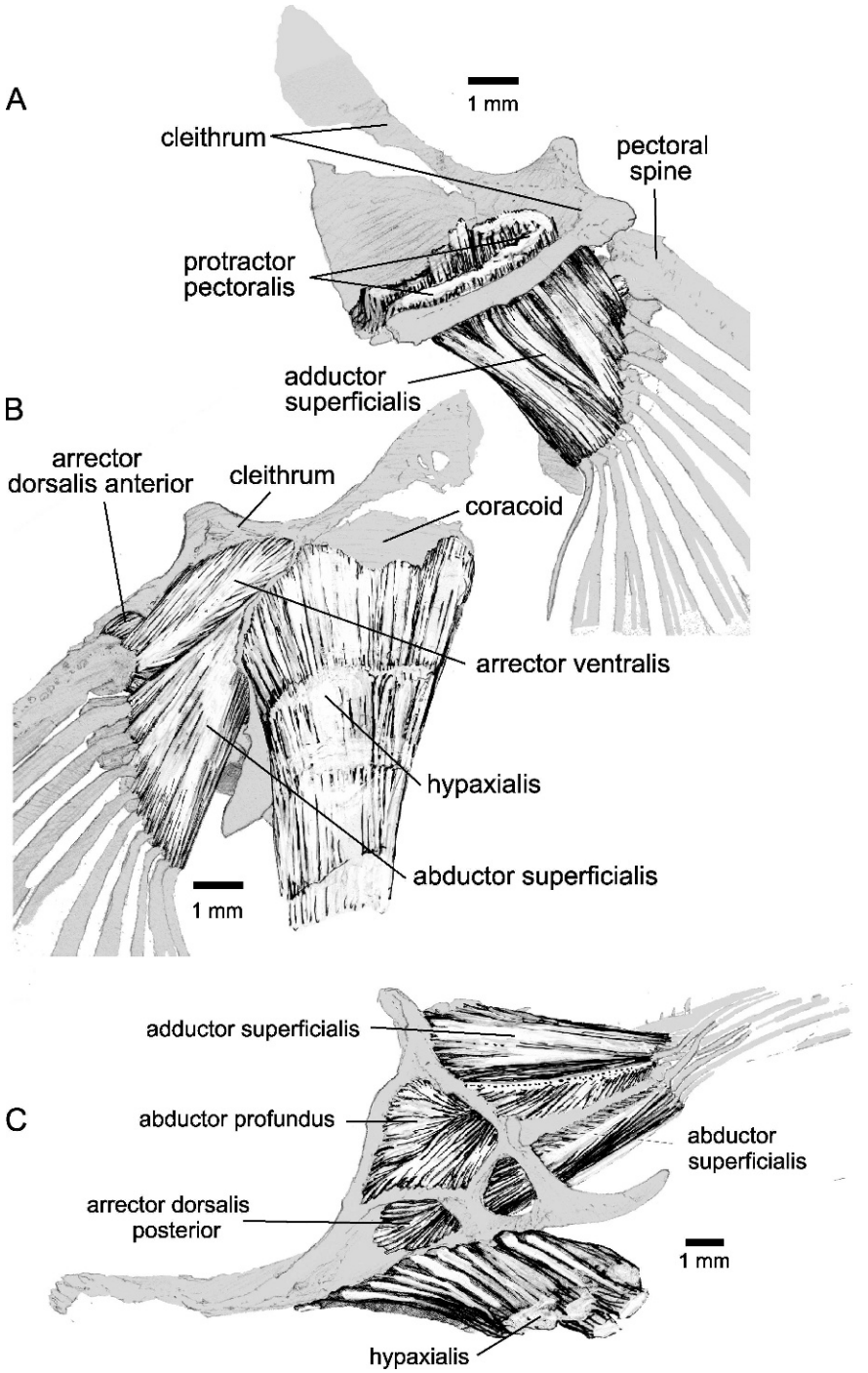

Fig. 25. Pectoral fin skeleton and musculature, *Lithogenes wahari*, right side. **A,** dorsal view; **B,** ventral view; **C,** mesial view. Scale is 1 mm. Drawings by Ian Hart.

ventralis (fig. 25B) short, triangular-shaped muscle between cleithrum and pectoral spine, occupying anteroventral position relative to other muscles of pectoral girdle. Origin is from ventral lamina of cleithrum along anterolateral margin of arrector fossa. Fibers originate broadly along fossa anterior margin, orient posterolaterally, pass ventral to the coracoid arrector bridge, and converge posteriorly to insert on narrow posteroventral process of pectoral-fin spine. Arrector dorsalis with separate anterior and posterior subdivisions. Anterior division a broad rectangular muscle between cleithrum and pectoral spine, occupying dorsal position relative to arrector ventralis. Origin is from ventral lamina of cleithrum along dorsal margin of arrector fossa. Fibers orient dorsolaterally, pass dorsal to the coracoid arrector bridge, to insert on the anterolateral head of the pectoral-fin spine. Posterior division narrow, elongate muscle between cleithrum and pectoral spine, lying dorsal to the arrector dorsalis ventral division. Origin is from the posteroventral cleithral lamina ventral to the origin of the abductor profundus muscle. Fibers of the arrector dorsalis posterior division pass through a channel (fig. 25C) formed by the cleithral lamina anteriorly and a mesial strut of the coracoid posteriorly; the latter separating the fibers of the arrector dorsalis dorsal division and the abductor profundus muscles. Insertion is on the anterior head of the pectoral spine, positioned dorsal and mesial to the spine insertion of the arrector dorsalis ventral division.

Abductor profundus a broad, thick muscle between cleithrum and pectoral spine, lying dorsal to the arrector dorsalis posterior division. Origin is from the posteroventral cleithral lamina. Fibers pass through a channel formed by the cleithral lamina anteriorly and the mesial and dorsal struts of the coracoid posteriorly. Insertion is on the dorsomedial condyle of the pectoral fin spine.

Adductor superficialis a broad, thick rectangular muscle between the cleithrum and pectoral fin rays. Origin is from the lateral margin of the dorsal process and lateral surface of the mesocoracoid arch. The muscle functions to elevate the fin relative to the horizontal plane and is subdivided, such that a thick dorsal division inserts on the anterodorsal aspect of the fin rays, thus serving also to abduct the fin rays, while a deeper division inserts on the posteroventral aspect of the fin rays and serves to adduct the fin rays.

Abductor superficialis, similar to adductor superficialis in configuration and function, lies between the coracoid and the fin rays and functions to de-elevate the fin relative to the horizontal plane. Origin is from the lateral margin of the coracoid humeral process and lateral surface of the medial mesacoracoid arch. The muscle is subdivided into mesial and ventral divisions, corresponding in form and function to those of the adductor superficialis.

Pelvic Fin

Pelvic fin i,4,i and without distal radials. First ray extremely thickened, depressed; hemitrichs separated along their entire length, bearing enlarged odontodes on ventral surfaces. Segmental lepidotrichs prominent, rectangular, becoming progressively smaller and more square distally. Unicuspid odontodes along entire length of medial hemitrich; odontodes on lateral hemitrich concentrated along lateral margin on distal half of fin ray. Proximal portion of the ventral surface of the first pelvic-fin ray without odontodes. Thickened skin of the pelvic pad forming extensive ridges. Fin rays 2–5 segmented and branched; last fin ray segmented, unbranched.

Paired basipterygia solid (fig. 26), with broadly expanded anterolateral processes and straight anterior margins, without medial processes. Antimeres strongly sutured to one another along midline on either side of an elongate, narrow synchondrosis. Lateral condyle for articulation with fin rays broad, convex. Lateral margin anterior to condyle produced as a slight ridge, or process. Posterior ischiac processes broadly expanded. Lateropterygium paddle shaped, its slender proximal end articulating indirectly via connective tissues with the basipterygium and head of lateral hemitrich of first fin ray. Lateropterygium greatly expanded distally, becoming progressively narrower toward blunt (smaller specimens) or pointed (larger specimens) tip; its greatest width at about midlength.

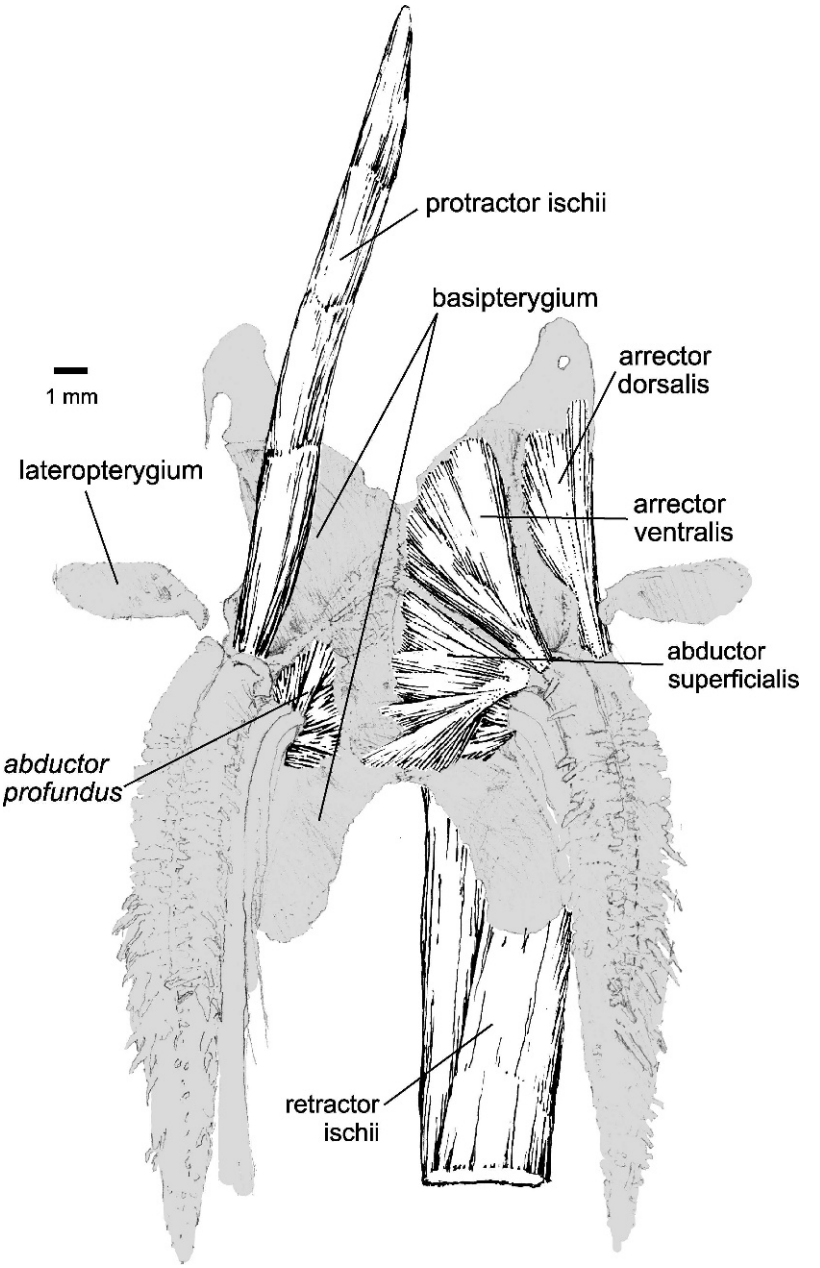

Fig. 26. Pelvic fin skeleton and musculature, *Lithogenes wahari*, ventral view. Ventral musculature removed from right side (left-hand portion of figure) to reveal abductor muscles. Scale is 1 mm. Drawing by Ian Hart.

Protractor ischii an elongate, narrow, strap-like muscle between the cleithrum and pelvic basipterygium. Unlike that of other loricariids and most siluriforms, the protractor ischii is a separate independent muscle, completely free from the hypaxialis musculature. The configuration differs from that in *Astroblepus*, which also shares an independent protractor ischii, in

that the muscle fibers are aligned parallel to the long axis of the muscle, as opposed to the spiral fiber orientation of astroblepids. Fibers are arranged in four muscle blocks, each separated by a distinct myocommata. Origin is from the ventral surface of the cleithrum at the symphysis; insertion is on the ventrolateral ridge of the basipterygium, medial to the articular process of the lateropterygium and ventral to the pelvic spine insertion of the arrector ventralis muscle.

Retractor ischii a thick, elongate muscle between the first anal-fin pterygiophore and the pelvic basipterygium. The muscle is separate and independent from the posterior hypaxialis muscles. Origin is from the dorsal surface of the pelvic basipterygium posterior process at a horizontal; through the lateral articular condyle for the thickened first pelvic ray and immediately ventral to the adductor profundus muscle. Insertion is onto the ventral surface of the expanded lateral process of the first anal-fin pterygiophore. Unlike the apomorphic condition in astroblepids, the fibers of the retractor ischii do not extend anteriorly to the anterior processes of the pelvic basipterygia.

Arrector dorsalis a short, narrow muscle between the basipterygium and first pelvic-fin ray. Its orientation is lateral and dorsal to the protractor ischii at the anterolateral margin of the basipterygium. Origin is from the dorsal lamina of the anterior basipterygium process; insertion is on the anteroventral corner of the lateral hemitrich of the thickened first pelvic-fin ray. The muscle is subdivided, wherein a small ventrolateral subdivision is apparent; its origin on the cartilagenous anterior portion of the basipterygium is positioned anterior to that of its larger median counterpart.

Arrector ventralis a broad, thin fan-shaped muscle between the basipterygium and the first pelvic-fin ray. Fibers originate broadly from the anterior half of the ventral lamina of the basipterygium. Fibers are oriented posterolaterally to converge onto a narrow tendinous insertion on the anteroventral margin of the medial hemitrich of the thickened first pelvic-fin ray.

Abductor superficialis divided into a number of separate bundles medially, some of which originate from the median basipterygium ridge of the contralateral side and alternate with like bundles of its antimere in an overlapping pattern. Fibers are oriented anterolaterally to converge on a tendinous insertion on the ventromedial process of the medial hemitrich of the first pelvic-fin ray.

Abductor profundus a broad, short rectangular muscle between the basipterygium and the ventral aspect of the branched pelvic-fin rays. The muscle lies between the ventral basipterygium lamina and the abductor superficialis muscle. Origin is from the posterior half of the basipterygium; insertion is on the ventromedial margins of pelvic-fin rays 2–6.

Adductor superficialis a broad, triangular muscle between the basipterygium and the first pelvic-fin ray. Origin is from the dorsal lamina of the anterioor half of the basipterygium. Fibers orient posterolaterally and converge to insert tendinously onto the dorsomedial process of the lateral hemitrich of the thickened first pelvic-fin ray.

Adductor profundus a short rectangular muscle between the basipterygium and the dorsomedial aspect of the branched pelvic fin rays. Origin is from the posterior half of the dorsal surface of the basipterygium; insertion is on the dorsomedial margins of pelvic-fin rays 2–6.

Dorsal Fin

Dorsal fin ii,6; supported internally by a total of eight pterygiophores, each ray associated with a discoid distal radial. First ray slender, unbranched; short, extending to about the midpoint of the length of the second ray. Proximal head of first ray flattened, expanded laterally and with slender lateral process; concave ventrally with cartilagenous articulation with concave facet of dorsoposterior aspect of second proximal radial. Robust ligament between anterior margin of first ray and posterodorsal process of first proximal radial; small discoid sesamoid ossification present in ligament, corresponding in position to ''first dorsal-fin spine'' of other loricariids. Second ray thickened, unbranched; articulating with blunt, square posterior process of second proximal radial. Third through eighth rays branched; each articulating with posterior process of corresponding proximal

radial. First proximal radial robust, with well-developed ventral midline lamina and expanded lateral laminae; its proximal end slender, articulating with an enlarged facet on posterodorsal margin of vertebra 7. Second proximal radial closely adpressed to first proximal radial along length of its anterior margin; lateral laminae well developed, with greatly expanded wings at point of dorsal spine articulation and with elongate lateral process that projects anterolaterally to directly contact proximal end of lateral bone. Third through sixth pterygiophores straight, relatively slender with small bilateral processes underlying articulation with distal radial, becoming progressively smaller posteriorly. Seventh and eighth pterygiophores without bilateral processes; last pterigiophore with enlarged bilateral wings directed caudad.

Anal Fin

Anal fin ii,6 or ii,6,i and supported internally by seven pterygiophores (fig. 27). First two rays unbranched, thickened relative to the shape of the more posterior fin rays. The proximal heads of the paired hemitrichs of the first ray are expanded and overlap the anterolateral portions of the proximal head of the second ray. The first two rays articulate with a small spherical distal radial that is borne by the first enlarged pterygiophore. Successive pterygiophores each articulate with a single fin ray and spherical distal radial, except for the posteriormost pterygiophore, which frequently, but not always, bears two fin rays, the posteriormost of which is unbranched. First pterygiophore enlarged, elongate, slightly concave; its proximal end articulating along ventral margin at junction of vertebrae 19 and 20. Proximal half of pterygiophore length nearly straight, bar shaped, with slightly expanded lateral shelves. Distal half of pterygiophore greatly expanded laterally, margins developed into broad lamina and rectangular distal processes; anterior and lateral margins concave, the latter the site of origin of enlarged retractor ischii. Successive more posterior pterygiophores slender, straight, without lateral lamina or processes. Posteriormost pterygiophore with an expanded lamina dorsal to its articulation with the fin rays.

The shape and configuration of the anal fin is sexually dimorphic. In males, the anterior margin of the fin is concave and each of the first five fin rays have a corresponding sigmoid shape. The first two (unbranched) rays are greatly thickened over the condition observed in females and juveniles. The first ray is notably shorter relative to the length of the rays in females and in the male the first ray is about half the length of the second ray. Each hemitrich bears a small process on its anterior margin. The flesh surrounding the thickened unbranched rays is bulbous and greatly thickened, with a lateral groove or sulcus between the first two fin rays. In both sexes, a paired slip of muscle separates off the main body of the hypaxialis to insert on the connective tissues surrounding the genital papilla.

Adipose Fin

Adipose fin low, elongate, triangular in shape; length approximately 3–4 times its height. Larger specimens with ossified slender spine embedding in flesh along anterior margin of fin and bearing numerous small odontodes along its entire length.

INTERRELATIONSHIPS AND BIOGEOGRAPHY

The relative paucity of discrete variation among the characters evaluated in this analysis presents a severe constraint in the determination of phylogenetic relationships among *Lithogenes* species at this time. Many of the characters observed to differ among species are uniquely derived and autapomorphic for one particular species and therefore are uninformative of interrelationships. These features were treated in the respective species accounts. Because *Lithogenes* species are known from so few specimens (except for abundant material of *L. wahari*), and because no tissue samples are available at present for analyses using DNA sequence variation, sources of character variation are restricted to morphological features that can be reliably compared from among ethanol-preserved and cleared and stained material. Other than a few externally visible conditions, it was not possi-

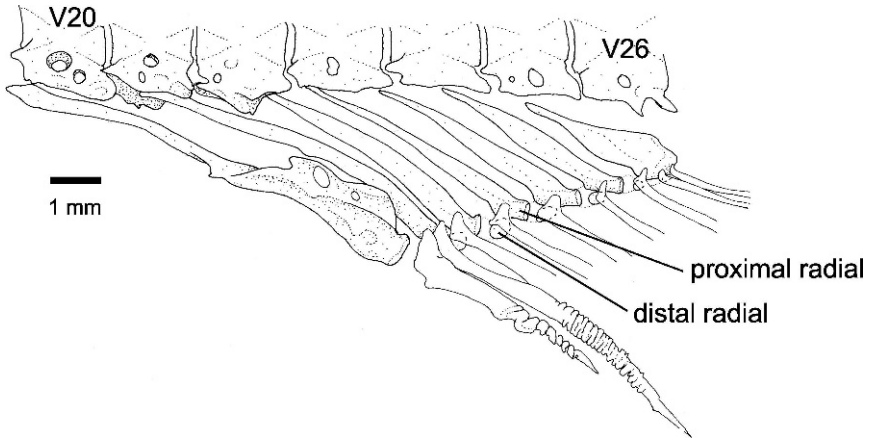

Fig. 27. Anal fin supports, *Lithogenes wahari*, left side, anterior toward left. Only the proximal portion of the branched fin rays is shown. Scale is 1 mm.

ble to evaluate myological features in a comparative framework because of the destructive sampling required by such analyses. Nevertheless, the following assessment is offered as a preliminary examination of species interrelationships.

The following characters used in the analysis are listed below, along with the condition and numerical code (in parentheses) observed for each taxon, and consistency index relative to the most parsimonious tree of relationships:

1. **Accessory premaxillary teeth**: absent (0)—*L. wahari*, *Astroblepus*, *Hemipsilichthys*; present (1)–*L. villosus*, *L. valencia*. CI = 0.5.
2. **Number of dentary teeth**: four or more (0)—*L. valencia*, *Astroblepus*, *Hemipsilichthys*; three or fewer (1)—*L. villosus*, *L. wahari*. CI = 1
3. **Hypertrophied cheek odontodes**: absent (0)—*L. villosus*, *Astroblepus*; present (1)— *Hemipsilichthys*, *L. valencia*, *L. wahari*. CI = 0.5.
4. **Suspensorium anterodorsal process**: absent (0)—*Astroblepus*, *Hemipsilichthys*; present on hyomandibula (1)—*L. valencia*; present on metapterygoid (2)—*L. villosus*, *L. wahari*. CI = 1.
5. **Lateral ethmoid extended caudally to orbit rim**: present (0)—*L. villosus*, *L. valencia*, *Astroblepus*; absent (1)—*L. wahari*, *Hemipsilichthys*. CI = 0.5.
6. **Lateropterygium shape**: discoid (0)—*L. wahari*, *Astroblepus*; slender (1)—*L. valencia*, *L. villosus*, *Hemipsilichthys*. CI = 0.5.
7. **Basipterygia anterior suture extent**: short, less than length of synchondrosis (0)—*Hemipsilichthys*, *Astroblepus*, *L. valencia*; elongate, greater than or equal to length of synchondrosis (1)—*L. villosus*, *L. wahari*. CI = 1.
8. **Total number of anal-fin rays**: seven (0)—*L. valencia*, *Astroblepus*, *Hemipsilichthys*; nine (1)—*L. wahari*, *L. villosus*. CI = 1.
9. **Preadipose plates**: present (0)—*L. villosus*, *L. valencia*, *Hemipsilichthys*; absent (1)—*L. wahari*, *Astroblepus*.

The results of the phylogenetic analysis are presented in figure 28. A single most-parsimonius tree was obtained, with tree length = 15, CI = 0.66, RI = 0.50. *Lithogenes villosus* is resolved as the sistergroup to *L.wahari* on the basis of four shared synapomorphies. Both species share reduction in the width and extent of the jaws, resulting in the derived reduction in the numbers of teeth carried by the jaw elements. *Lithogenes valencia* shares very broad jaw elements bearing numerous teeth with the outgroups. *Lithogenes villosus* and *L. wahari* share the presence of the suspensorial posterodorsal process on the metapterygoid, versus the presence of a putatively homologous process on the hyomandibula in *L. valencia*. In *L. villosus* and *L. wahari*, the

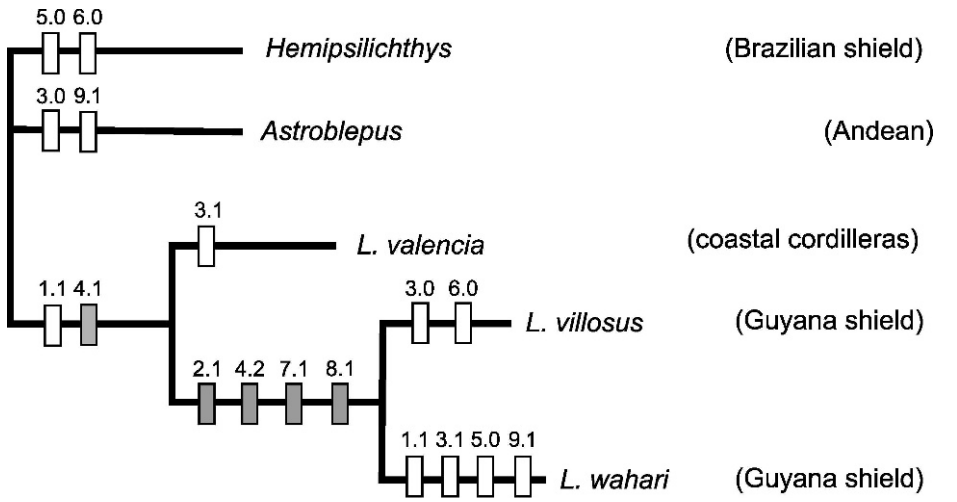

Fig. 28. Results of the phylogenetic analysis among *Lithogenes* species. Single most-parsimonious tree topology and geographic distribution of included taxa, outgroup node collapsed, tree length 15 steps, CI = 0.66, RI = 0.44. Solid rectangles designate unreversed synapomorphy, open rectangles designate homoplastic character-state change. Characters are numbered as described in text, decimal component denotes the character state.

anterior suture joining antimeres of the pelvic-fin basipterygium is elongate relative to the length of that suture in *L. valencia* and outgroups. Finally, *L. villosus* and *L. wahari* share nine anal-fin rays, whereas *L. valencia* and outgroups have seven or fewer.

Both *L. villosus* and *L. wahari*, recovered as sister taxa in the phylogenetic analysis (fig. 28), occur in rivers of the Guyana Shield of northern South America. All three *Lithogenes* species are known at present from single localities. *Lithogenes valencia* is known only from the endorheic Lago Valencia region situated within the Cordillera de la Costa region of northern Venezuela. Astroblepid catfishes are exclusively Andean in distribution and do not occur in the coastal cordilleras of Venezuela, the Guyana Shield, or in the lowlands of the Amazon or Orinoco basins. There is no fossil record for the Lithogeninae or the Astroblepidae.

The pattern of phylogenetic relationships among lithogenine species, when compared to their current distributions (fig. 28), suggests an ancestral widespread distribution for the Lithogeninae throughout the Guyana Shield plus the Cordillera de la Costa of northern South America that was in place by Eocene (50–60 Ma) time. The formation of the Cordillera de la Costa pre-dates the Miocene (8–10 Ma) uplift of the Merida Andes and is thought to be associated with collision of the Caribbean Plate with the Bahamian platform (Pindell and Barrett, 1990) beginning in the Late Cretaceous (70–78 Ma), with continued uplift via accretion of the Carribean Plate onto the South American Plate through the Miocene (Smith et al., 1999). Later, perhaps no later than the early to middle Miocene, the region between the Cordillera de la Costa and the Guyana Shield became epicontinental sea, as indicated by the sediments of the Chaguaramas, Oficina, and Carapita formations (Pérez de Mejía et al., 1980). The biogeographic pattern thus described by lithogenine species relationships is congruent with a hypothesis of vicariance and divergence of *L. valencia* from the Guyana Shield endemic species, resulting from early to mid-Miocene development of transitional deltaic to fully marine environments in the Guarico and Maturin basins occupying the region between the coastal ranges and Guyana Shield.

This biogeographic hypothesis requires that lithogenine catfishes were extant and widespread prior to the events responsible for the formation of the coastal mountain ranges and subsequent isolation of the Caribbean coastal

freshwater fish fauna. In contrast, a somewhat younger and better documented biogeographic pattern of sister-clades occurring on either side of the mountains that now separate the Maracaibo and coastal drainages from the Orinoco basin is common among Neotropical fishes (summarized in Albert et al., 2006). For example, the distribution of species of the loricariid genus *Chaetostoma* (throughout Andean, Guyana Shield, and Caribbean coastal regions; Lasso and Provenzano, 1997) suggests a common ancestral widespread distribution perhaps as old as that suggested by lithogenine loricariids. However, we are aware of no other examples of fishes sharing a Caribbean coastal plus Guyana Shield distribution. The closest example of this particular biogeographic pattern that we are aware of, although based on a single species distribution, is provided by the curimatid *Steindachnerina argentea*, which is distributed in both the Caribbean coastal region and the Guyana Shield, plus the island of Trinidad (Vari, 1991). The paucity of corroborating distributions involving other freshwater fishes is perhaps not surprising, given that the fish fauna of the Caribbean coastal region is relatively depauperate. On the other hand, the Maracaibo fauna is comparatively much richer and yet more complex in the historical derivation of its ichthyofauna (Albert et al., 2006). On that basis, one could expect that remnants of vicariance involving widespread faunas in these regions would be more prevalent. There is no fossil record to verify that lithogenines had a widespread distribution throughout intervening regions between the Guyana Shield and northern Venezuela, nor are their estimates of DNA sequence divergence of *Lithogenes* from their loricariid sistergroup to establish an independent temporal framework for the historical biogeographic hypothesis suggested herein. However, available phylogenetic evidence does not invalidate the idea that lithogenines are at least early Eocene or older in age. Phylogenetic evidence places lithogenines as the sister group to all other Loricariidae (Schaefer, 2003). Loricariids are members of the Loricarioidea, which was recovered as the sister group to all other catfishes in the phylogenetic analysis of Sullivan et al. (2006). This result, in combination with the existence of the Paleocene fossil callichthyid *Corydoras revelatus* (Cockerell, 1925; Reis, 1998), points to a relatively ancient age for the divergence of lithogenines from other loricariids.

ACKNOWLEDGMENTS

We thank the following individuals and institutions for the loan and exchange of specimens and information: M. Sabaj and J. Lundberg (ANSP), J. Armbruster (AUM), W. Eschmeyer and D. Catania (CAS), Barry Chernoff, M. Westneat, and M. Rogers (FMNH), Roberto Reis and E. Pereira (MCP). Radford Arrindell, Barbara Brown, and Luis Fernandez (AMNH) provided technical assistance; myology drawings were prepared by Ian Hart. Fieldwork activities in Venezuela were supported by a grant to S. Schaefer from the Constantine S. Niarchos Scientific Expedition Fund; S. Schaefer was further supported by NSF award DEB-0314849. Roberto Reis and Donald Taphorn offered helpful comments on the manuscript. We thank Jonathan Baskin, Angel Rojas, and the people of the community of Raudal El Danto, Amazonas State, Venezuela, for assistance in the field.

REFERENCES

Adams, D.C., F.J. Rohlf, and D.E. Slice. 2004. Geometric morphometrics: ten years of progress following the 'revolution'. Italian Journal of Zoology 71: 5–16.

Albert, J.S., N.R. Lovejoy, and W.G.R. Crampton. 2006. Miocene tectonism and the separation of cis- and trans-Andean river basins: evidence from Neotropical fishes. Journal of South American Earth Sciences 21: 14–27.

Bhatti, H.K. 1938. The integument and dermal skeleton of Siluroidea. Transactions of the Zoological Society of London 24: 1–79.

Cockerell, T.D.A. 1925. The fossil fish of the family Callichthyidae. Science 62: 397–398.

Eigenmann, C.H. 1909. Reports on the expedition to British Guiana of the Indiana University and the Carnegie Museum, 1908. Report no. 1. Some new genera and species of fishes from British Guiana. Annals of Carnegie Museum 6(1): 4–54.

Evermann, B.W., and W.C. Kendall. 1905. An interesting species of fish from the high Andes of central Ecuador. Proceedings of the Biological Society of Washington 18: 91–105.

Geerinckx, T. 2007. Ontogeny and functional morphology of a highly specialized trophic apparatus: a case study of neotropical suckermouth armoured catfishes (Loricariidae, Siluriformes). Unpublished Ph.D. dissertation, Universiteit Gent, Belgium, I. text: i–iii + 244 pp.; II: figs.: 99 pp.

Goloboff, P.A. 1999. NONA, ver. 2.0: Distributed by J. Carpenter, AMNH.

Gosline, W.A. 1947. Contributions to the classification of the loricariid catfishes. Arquivos do Museu Nacional Rio de Janeiro 41: 79–134.

Hardman, M., L.M. Page, M.H. Sabaj, J.W. Armbruster, and J.H. Knouft. 2002. A comparison of fish surveys made in 1908 and 1998 of the Potaro, Essequibo, Demerara, and coastal river drainages of Guyana. Ichthyological Exploration of Freshwaters 13(3): 225–238.

Howes, G.J. 1983. The cranial muscles of loricarioid catfishes, their homologies and value as taxonomic characters (Teleostei: Siluroidei). Bulletin of the British Museum (Natural History) Zoology 45: 309–345.

Johnson, R.D.O. 1912. Notes on the habits of a climbing catfish (*Arges marmoratus*) from the Republic of Colombia. Annals of New York Academy of Science 22: 327–333.

Lasso, C.A., and F. Provenzano. 1997. *Chaetostoma vasquezi*, nueva especies de corroncho del Escudo de Guayana, Estado Bolívar, Venezuela (Siluroidei: Loricariidae): descripción y consideraciones biogeográficas. Memoria Sociedad de Ciencias Naturales La Salle 62: 53–65.

Lundberg, J.G., and J.N. Baskin. 1969. The caudal skeleton of the catfishes, order Siluriformes. American Museum Novitates 2398: 1–49.

Macdonnell, A.J., and R.W. Blake. 1990. Rheotaxis in *Otocinclus* sp. (Teleostei: Loricariidae). Canadian Journal of Zoology 68: 599–601.

Nijssen, H., and I.J.H. Isbrücker. 1987. *Spectracanthicus murinus*, nouveaux genre et espèce de Poisson-Chat cuirassé du Rio Tapajós, Est. Pará, Brésil, avec des remarques sur d'autres genres de Loricariidés (Pisces, Siluriformes, Loricariidae). Revue Française d'Aquariologie et Herpétologie 13: 93–98.

Nixon, K.C. 2002. WinClada, ver. 1.00.08. Ithaca, NY: Distributed by the author.

Pérez de Mejía, D., G.D. Kiser, B. Maximowitsch, and G. Young. 1980. Geología de Venezuela. *In* B. Felder, A. Brie, J. Gartner, V. Hepp, M. Hrabie, M. Kervella, F. Mons, G. Mowat, N. Neville, J. Plomb, W. Sadras, A. Tejada, J. Trassard, J. Vidal and D. Zinat (editors), Evaluación de Formaciones en Venezuela. Caracas, Venezuela: Schlumberger Surenco S.A., 1–44.

Pindell, J.L., and S.F. Barrett. 1990. Geological evolution of the Caribbean region: a plate-tectonic perspective. *In* G. Dengo and J.E. Case (editors), The Caribbean region. Geology of North America Vol. H. Boulder, CO: Geological Society of America, 405–432.

Provenzano, F., S.A. Schaefer, J.N. Baskin, and R. Royero-Leon. 2003. New, possibly extinct lithogenine loricariid (Siluriformes, Loricariidae) from northern Venezuela. Copeia 2003: 562–575.

Reis, R.E. 1998. Systematics, biogeography, and the fossil records of the Callichthyidae: a review of the available data. *In* L.R. Malabarba, R.E. Reis, R.P. Vari, C.A.S. Lucena and Z.M.S. Lucena (editors), Phylogeny and classification of Neotropical fishes. Porto Alegre, Brazil: Edipucrs, 351–362.

Reis, R.E., S.O. Kullander, and C.J. Ferraris. 2003. Family Loricariidae. *In* R.E. Reis, S.O. Kullander and C.J. Ferraris (editors), Checklist of the freshwater fishes of South and Central America. Porto Alegre, Brazil: Edipucrs, 318 pp.

Rohlf, F.J., and D. Slice. 1990. Extension of the Procrustes method for the optimal superimposition of landmarks. Systematic Zoology 39: 40–59.

Schaefer, S.A. 1987. Osteology of *Hypostomus plecostomus* (Linnaeus), with a phylogenetic analysis of the loricariid subfamilies (Pisces: Siluroidei). Natural History Museum of Los Angeles County Contributions in Science 394: 1–31.

Schaefer, S.A. 1997. The Neotropical Cascudinhos: systematics and biogeography of the *Otocinclus* catfishes (Siluriformes: Loricariidae). Proceedings of the Academy of Natural Sciences of Philadelphia 148: 1–120.

Schaefer, S.A. 2003. Relationships of *Lithogenes villosus* Eigenmann, 1909 (Siluriformes, Loricariidae): evidence from high-resolution computed microtomography. American Museum Novitates 3401: 1–55.

Schaefer, S.A., and A.E. Aquino. 2000. Postotic laterosensory canal and pterotic branch homology in catfishes. Journal of Morphology 246: 212–227.

Schaefer, S.A., and G.V. Lauder. 1986. Historical transformation of functional design: evolutionary morphology of feeding mechanisms in loricarioid catfishes. Systematic Zoology 35: 489–508.

Shelden, F.F. 1937. Osteology, myology, and probable evolution of the nematognath pelvic girdle. Annals of New York Academy of Sciences 37: 1–96.

Smith, C.A., V.B. Sisson, H.G. Avé Lallemant, and P. Copeland. 1999. Two contrasting pressure-temperature-time paths in the Villa de Cura bleuschist belt, Venezuela; possible evidence for Late Cretaceous initiation of subduction in the Caribbean. Geological Society of America Bulletin 111: 831–848.

Springer, V.G., and G.D. Johnson. 2000. Use and advantages of ethanol solution of alizarin red S dye for staining bone in fishes. Copeia 2000: 300–301.

Springer, V.G., and G.D. Johnson. 2004. Study of the dorsal gill-arch musculature of teleostome fishes, with special reference to the Actinopterygii. Bulletin of the Biological Society of Washington 11: 1–260 + 206 pls.

Sullivan, J.P., J.G. Lundberg, and M. Hardman. 2006. A phylogenetic analysis of the major groups of catfishes (Teleostei: Siluriformes) using *rag1* and *rag2* nuclear gene sequences. Molecular Phylogenetics and Evolution 41: 636–662.

Taylor, W.R., and G.C. Van Dyke. 1985. Revised procedures for staining and clearing small fishes and other vertebrates for bone and cartilage study. Cybium 9: 107–119.

Vari, R.P. 1991. Systematics of the Neotropical characiform genus *Steindachnerina* Fowler (Pisces: Ostariophysi). Smithsonian Contributions to Zoology 507: 1–118.

Winterbottom, R. 1974. A descriptive synonymy of the striated muscles of the Teleostei. Proceedings of the Academy of Natural Sciences of Philadelphia 125: 225–317.

Complete lists of all issues of the *Novitates* and the *Bulletin* are available at World Wide Web site http://library.amnh.org/pubs. Inquire about ordering printed copies via e-mail from scipubs@amnh.org or via standard mail from: American Museum of Natural History, Library—Scientific Publications, Central Park West at 79th St., New York, NY 10024. TEL: (212) 769-5545. FAX: (212) 769-5009.

This paper meets the requirements of ANSI/NISO Z39.48-1992 (Permanence of Paper).